Location: About 200 m north-northwest of Sherlock crater.
Illustrations: Figure 236.
Comments: Sample is regolith material of the cluster ejecta.
Petrograhic descriptions: 70320-24, dominantly basalt and breccia fragments with some glass and agglutinates.

GEOLOGIC SYNTHESIS

GENERAL SETTING AND HISTORICAL FRAMEWORK

The geologic setting and stratigraphic framework, interpreted after the Apollo 17 mission, have been discussed in several previous papers (Muehlberger and others, 1973; Apollo Field Geology Investigation Team, 1973; Reed and Wolfe, 1975; Wolfe and others, 1975; Wolfe and Reed, 1976). These are recapitulated and amplified in the following pages largely without further citation.

Briefly, we envision the massifs as the upper part of thick ejecta deposited on the rim of the transient cavity of the large southern Serenitatis basin, which was formed about 3.9 to 4.0 b.y. ago by the impact of a planetesimal. The ring structure and the approximately radial grabens that give the massif blocks definition were imposed on the ejecta blanket before deposition of the knobby-textured Sculptured Hills material. The mountainous terrain thus formed was partly flooded by the subfloor basalt, and the general region was mantled by a thin volcanic ash unit. After gentle warping and tensional faulting in the Taurus-Littrow area, younger basalts were extruded to the west within Mare Serenitatis (pl. 1). During approximately the last 3.5 b.y., since deposition of the volcanic ash, continued bombardment by meteorites and secondary projectiles has produced a thick regolith. Relatively late in this interval, the Lee-Lincoln fault scarp resulted from structural adjustments. About 100 m.y. ago a swam of secondary projectiles from Tycho formed the large cluster of craters east and south of the landing point (pl. 2); when the Tycho projectiles struck the north face of the South Massif, they mobilized fine-grained regolith material, which was redeposited on the valley floor as the light mantle. Small extensional faults cut the light mantle (pl. 2).

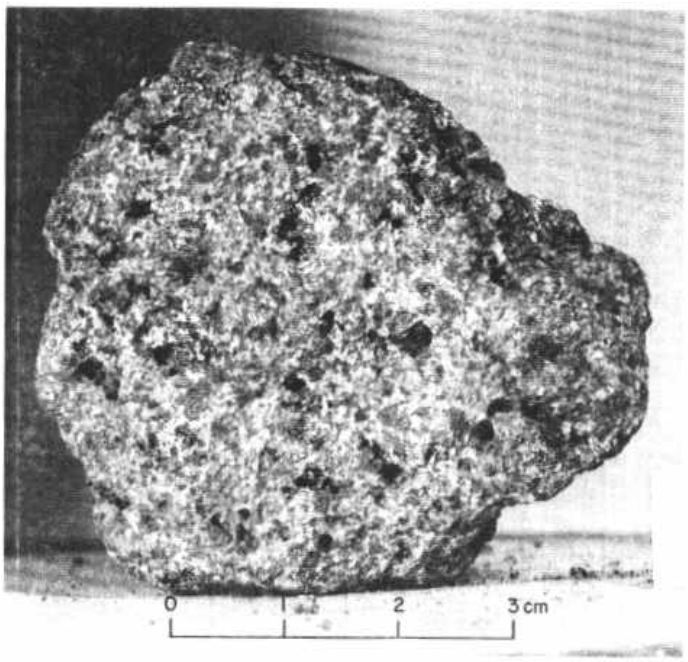

FIGURE 237.- Sample 70315. Medium-grained vesicular basalt.
(NASA photograph S-73-15453.)

SOU'T'HERN SERENITATS BASIN STRUCTURE

On the basis of orbital gravity data (Sjogren and others, 1974a) and geologic interpretation, Scott (1974) suggested that two basins underlie Mare Serenitatis. The larger, more southerly basin is centered at approximately lat 24.5°N, long 18°E. Extending Scott's (1974) interpretation and modifying the ring structure previously shown by Wilhelms and McCauley (1971) for a single basin (fig. 3), Wolfe and Reed (1976) proposed a revised ring structure (fig. 238).

Ring 1 is represented by prominent wrinkle ridges whose distribution approximates a circle with a 200-km radius (Scott, 1974). Muehlberger (1974) suggested that a wrinkle ridge of this sort may be developed in the mare basalt where a drowned ring of the basin structure affects the compressional stress field that produced the ridges.

Ring 2 is represented by the arc of the Haemus Mountains. Extended to the northeast with the 290-km radius measured from the basin center to the Haemus Mountains, ring 2 underlies the basalt of easternmost Mare Serenitatis (fig. 238).

Fitting ring 3 to Scott's (1974) basin center, Wolfe and Reed (1976) connected segments of the second and third rings previously shown by Wilhelms and McCauley (1971) for a single Serenitatis basin (fig. 3). The connecting segment passes approximately through the Apollo 17 landing area (fig. 238).

Wilhelms and McCauley (1971) identified a fourth ring with a radius of about 670 km in the highlands southwest of Mare Serenitatis (figs. 3 and 238). Their third ring (fig. 3) lies about 530 km east of the southern Serenitatis basin center. It is difficult to say whether either of these segments represents a basin rim analogous to the fourth ring (Cordillera Mountains) of the Orientale basin or to the outer ring (Apennine Mountains) of the Imbrium basin. Such an outer ring may never have been well developed in the southern Serenitatis basin structure or may have been

largely obliterated by subsequent events.

The rings of the southern Serenitatis basin structure are correlated with those of the better preserved Orientale basin structure as shown in table 5. The correlation derives particular support from morphologic similarities suggesting that the outer Rook ring (ring 3 of the Orientale basin) and the Littrow ring (ring 3 of the southern Serenitatis basin) are analogous structures. The Rook Mountains in the southeastern part of the Orientale basin and the Apollo 17 landing area southeast of Mare Serenitatis are shown in orbital view at similar scale in figures 239 and 240. In each area, several massifs of similar shape and size are crudely alined along trends radial to the basin centers, and linear grabenlike troughs approximately radial to the basin centers cut through the mountainous third rings. In the Apollo 17 area, mare basalt has flooded such troughs and buried the lower parts of the massifs.

The spatial relations in both basins of the massifs to the knobby terrain provides further support for the correlation of basin structures. The knobby-textured terrain of the Orientale basin (knobby basin material of Moore and others (1974); domical facies of Head (1974b); knobby facies of the Rook Formation of Scott and others (1977)) occurs in the grabenlike trough that transects the outer Rook ring (fig. 239) and extends over most of the surface between the Rook Mountains

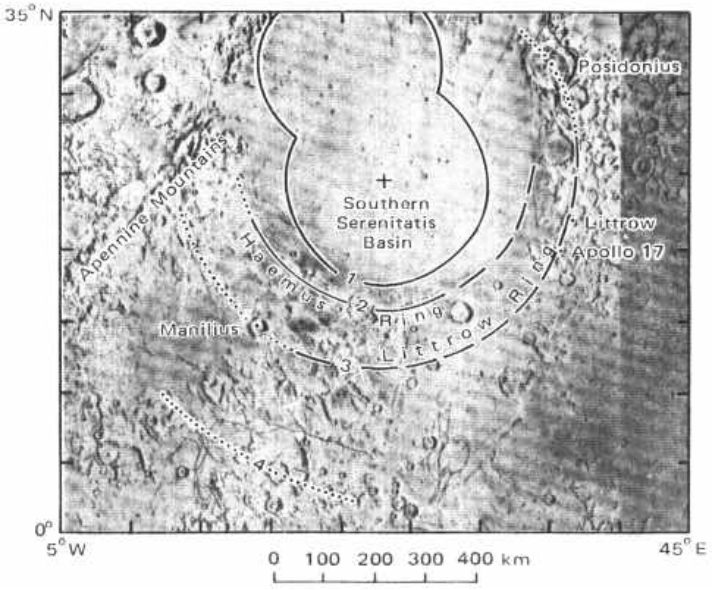

FIGURE 238.-Revised ring structure of Mare Serenitatis area. Solid line segments from Scott (1974); dotted-line segments froth Wilhelms and McCauley (1971); dashed-line segments from Wolfe and Reed (1976). Cross shows approximate center of southern Serenitatis basin Numbers 1 through 4 identify basin rings discussed in text. Compare with figure 3. (From Wolfe and Reed, 1976.)

TABLE 5.-*Comparison of southern Serenitatis and Orientale basin structures*

Data for Orientale basin except as indicated from Moore and others (1974).

	Southern Serentatis basin – Structure radii (kilometers)	Orientale basin-structure radii (kilometers)	Ratio of radii
Ring 1	200	160	1.25
Ring 2	290 (Haemus ring)	240 (inner Rook riing)	1.21
Ring 3	375 (Littrow ring)	300 (outer Rook ring)	1.25
Ring 4	650?	450 (Cordillera riing)	1.44
Mascon (calculated surface disk)	[1]221	[2]150	1.5

[1]Sjoren and others (1974)b.
[2]Scott (1974)

and the scarp that forms the basinward face of the Cordillera Mountains (fig. 241). Comparable knobbytextured Sculptured Hills terrain forms a major part of the highlands adjacent to eastern Mare Serenitatis (fig. 240; pl. 1). It partly surrounds the Taurus-Littrow massifs much as its Orientale counterpart surrounds the Rook Mountain massifs, and it projects locally through the mare basalts that floor the grabenlike valleys. Head (1974a) made a similar correlation of the massifs and Sculptured Hills of the Apollo 17 region with the Alpes Mountains and Alpes Formation of the Imbrium basin.

Head (1974b) noted the predominance of knobby terrain at Orientale, between the Rook Mountains and the Cordillera scarp, and interpreted it as lineated ejecta on which the knobby or domical texture was imposed by seismic shaking during formation of the Cordillera scarp. In more recent mapping, Scott and others (1977) have interpreted the knobby-terrain material as an ejecta unit that is partly confined by the preexisting Cordillera scarp; where it overlaps the scarp, the knobby unit overlies the radially lineated Hevelius Formation, also interpreted as ejecta. Supporting evidence for the hypothesis that the knobbyterrain material is a discrete little-modified basinejecta unit comes from the Imbrium basin. Knobbyterrain material (Alpes Formation) occupies an extensive area within the Apennine ring in the northeast quadrant of the lmbrium basin. It also extends hundreds of kilometers, mainly east and south of the limits of the Imbrium ring structure (Wilhelms and McCauley, 1071). This distribution is a likely one for basin ejecta but is unlikely for a texture imposed on preexisting materials by seismic shaking associated with formation of the Apennine scarp. Distribution of the knobby-terrain material with respect to grabens, massifs, radially lineated ejecta, and basin-forming scarps, as outlined above, suggests that the knobby terrain material is ejecta that was emplaced during basin formation but after development of the ring structure and the grabens.

SIGNIFIGANCE OF THE THIRD RING

Assuming that the massifs and Sculptured Hills of the Taurus-Littrow area are genetic as well as morphologic analogs of the Rook Mountain massifs and knobby terrain of the Orientale basin, we can apply concepts to the Taurus-Littrow region that were developed froth studies of the better preserved Orientale basin.

Several recent workers (Baldwin, 1972; McGetchin and others, 1973; Moore and others, 1974; Head, 1974b; McCauley, 1977) have suggested that the Rook Mountains are located approximately at the rim of the initial crater-the so-called transient cavity-that was excavated by basin-forming impact. Photogeologic support for this hypothesis has been developed by Head (1974b), who by analogy with the large crater Hausen (170 km in diameter) and the Schrodinger basin (320 km in diameter) suggested that the inner Rook ring (ring 2, table 5) is a central peak ring and that the outer Rook ring is the approximate rim of the transient cavity. Drawing on photogeologic interpretation of the Orientale basin and on data from terrestrial explosion craters. McCauley (1977) also concluded that the inner Rook ring is a central peak ring and that the Rook mountain massif's represent the crest of the transient cavity rim.

We believe that the transient cavity in a multi-ring basin briefly approaches the bowl shape of a small lunar impact crater. However, the lunar crust and mantle lack the strength to maintain an open hole of such proportions; rapid modification occurs due to immediate isostatic adjustment and to centripetal movement of crust and mantle materials toward the transient cavity. McCauley (1977) has attributed formation of the Cordillera scarp (fig. 241) to such centripetal movement during the basin-forming event.

Moore and others (1974), in estimating thickness of ejecta from the calculated depths of buried craters, determined a thickness of 2-4 km of Orientate ejecta at the crest of the Cordillera ring. Plotting their empirical estimates of' thickness against distance from the basin center, they selected the equation of McGetchin and others (1973) as a reasonable fit to their data for a transient cavity of 300-km radius. The equation is $t=T(r/R)^{-3}$, where T is the thickness of ejecta at the initial crater rim, R the radius of the initial crater. and t the thickness of ejecta at distance r, measured from the center of the crater. As fit to the empirical data by Moore and others. this equation predicts 12 km of

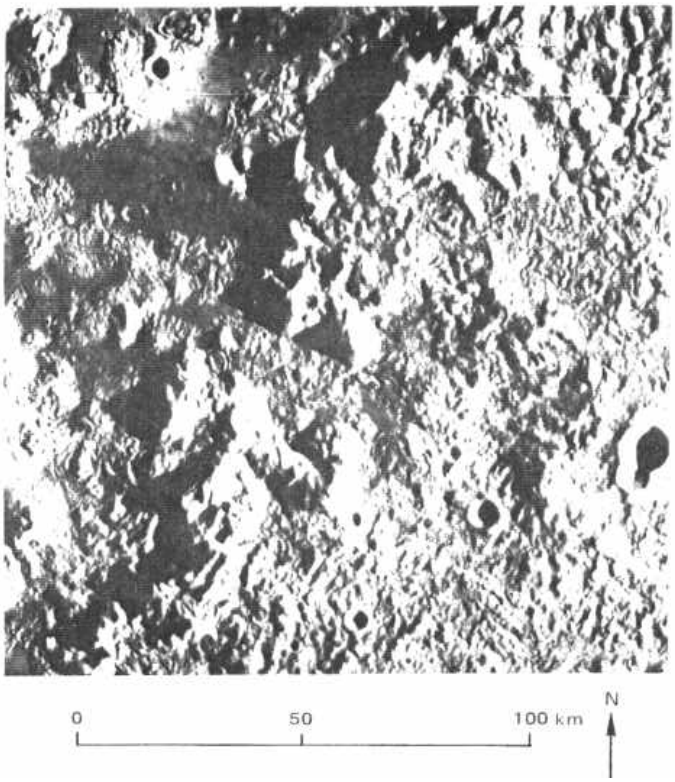

FIGURE 239.-Rook Mountains in the southeastern quadrant of the Orientate basin. Location of this area is shown in figure 241. (Lunar Orbiter IV high-resolution frame 181.) (From Wolfe and Reed, 1976.)

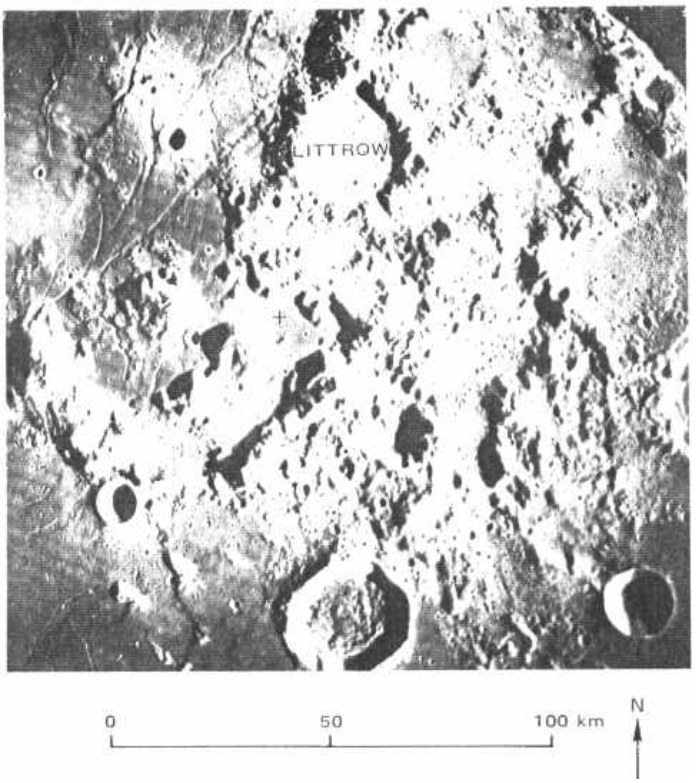

FIGURE 240-Mountainous terrain southeast of Mare Serenitatis in the Apollo 17 region. Cross shows Apollo 17 landing point. (Mapping-camera photograph AS 17-M-446.) (From Wolfe and Reed, l976.)

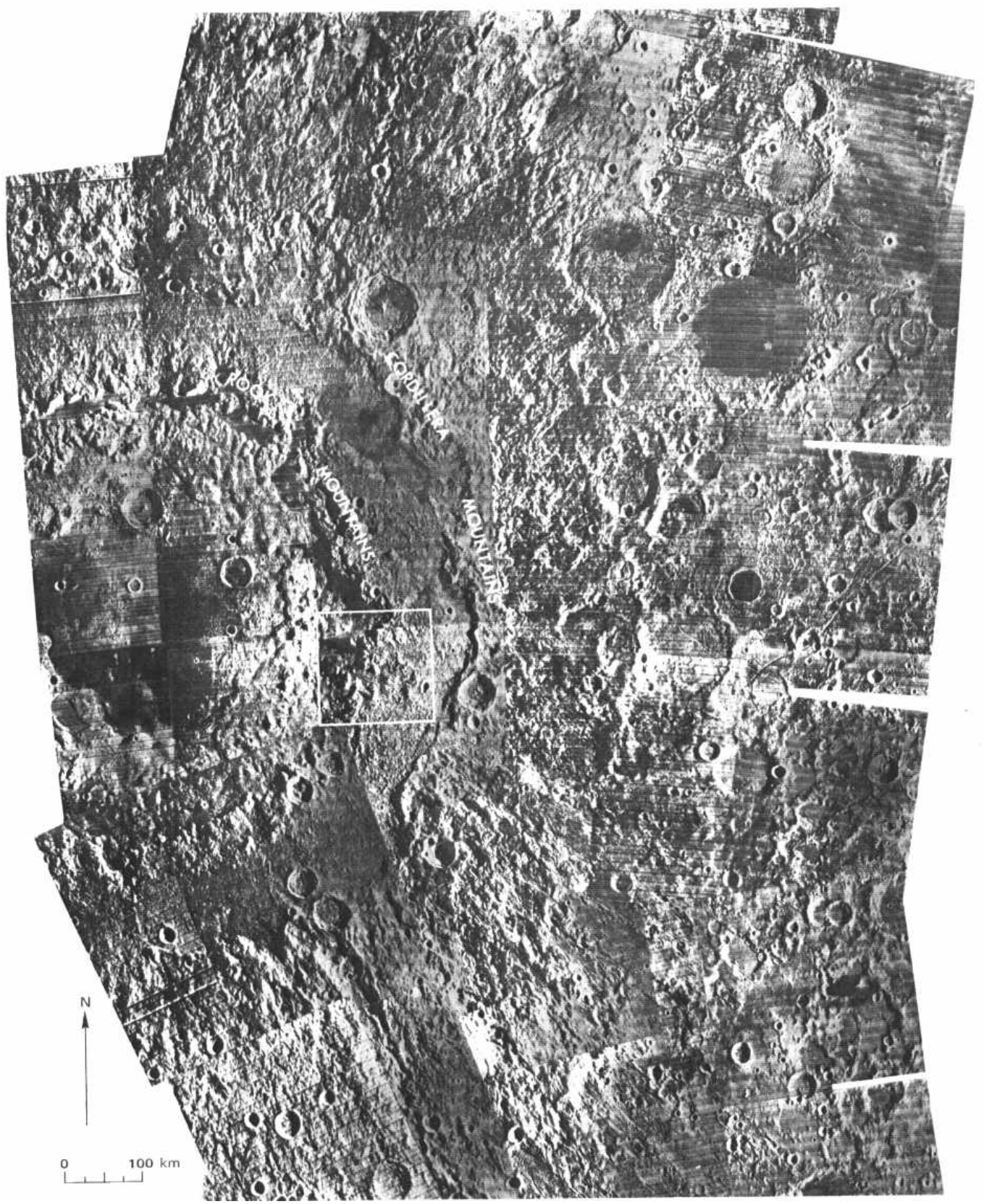

FIGURE 241.-Eastern part of Orientale basin. Square shows location of figure 239. (Uncontrolled mosaic of Lunar Orbiter IV highresolution images.) (From Wolfe and Reed, 1976.)

ejecta at the rim of the Orientale transient cavity and 3.6 km at a position equivalent to the Cordillera ring. Moore and others (1974) further pointed out that another equation of McGetchin and others (1973), for small experimental craters ($T=0.04R$, notation as above), predicts 12 km of ejecta at the rim of a transient crater 300 km in radius. Whether or not the calculated thicknesses are precisely correct, the ejecta at the outer Rook ring must be thicker than the 2-4 km determined empirically at the Cordillera crest.

The two equations (above) used by Moore and others (1974) are for craters with the shapes of small impact craters. Support for the assumption that the transient cavity approaches the shape of a small impact crater comes from comparison of ejecta volumes calculated from crater geometry and from interpretation of gravity data. Using the equation of McGetchin and others (1973) for cumulative volume (V) at distances of r and greater ($V=2_{II}TR^2(R/r)$, notation as above) and using R=300 km, T=12 km, Moore and others (1974) calculated the total volume of Orientale ejecta beyond the Cordillera rim to be about $4.5x10^6$ km^3, a value in reasonable agreement with the $5.3x10^6$ km^3 estimated by Scott (1974) from interpretation of gravity data. These estimates of Orientale ejecta volume are significantly greater than the $1.0\text{-}2.0x10^6$ km^3 that Head and others (1975) have suggested as a preferred estimate. In fact, when ejecta volume between the Rook Mountains and Cordillera scarp is included, the estimate of Moore and others is $6.8x10^6$ km3.

With respect to their much smaller estimates of volume, Head and others (1975) have suggested that the depth of excavation of Orientale was 6-14 km. Moore and others (1974), in contrast, applied Pike's equations for experimental craters ($a=0.225D^{0.96}$ and $h=0.043D^{0.91}$, where a is the depth of the crater measured from the rim crest, h is the height of the rim above the local surroundings, and D is the diameter of the crater; all variables in kilometers) to estimate that the Orientate transient crater was about 85 km deep. It may have excavated a small amount of material from the lunar mantle (depth greater than 60 km).

Extrapolation to the slightly larger southern Serenitatis basin (table 5) suggests that the transient crater may have been more than 100 km deep and that many kilometers of ejecta was emplaced in the vicinity of the Apollo 17 landing site. The relation T=0.048, which predicts 12 km of ejecta at the rim of the Orientate transient cavity, suggests a thickness of 15 km at the rim of the southern Serenitatis transient cavity. Even if this estimate is several times too large, the thickness of southern Serenitatis basin ejecta would exceed the height of the exposed faces of the massifs from which samples were collected. Later, but still during the period of basin formation, the ring structure and radial faults that define the massifs were imposed on the ejecta.

STRATIGRAPHY OF THE TAURUS-LITTROW VALLEY

MASSIFS

The linearity of the Taurus-Littrow valley walls implies that the bounding faults, generated during formation of the southern Serenitatis basin, are steeply diping. These faults are not now exposed. Perhaps the segment of the Lee-Lincoln scarp on the North Massif follows the zone of weakness along such a fault. Initially, high-angle fault surfaces formed oversteep massif slopes that must have been unstable and collapsed almost immediately to form wedges of colluvium along their lower parts (fig. 242) . The bulk of the colluvium probably accumulated as the graben was forming. However, partial filling of Nansen crater shows that mass wasting has continued into recent time.

The massifs as mapped (pls. 1 and 2) include bedrock with a veneer of regolith on the upper slopes and, on the. lower slopes, the upper parts of the colluvial wedges (fig. 242). Stations 2, 6, and 7 are on the colluvial wedges. The large boulders sampled at each of these stations rolled down over the wedges from the higher parts of the massifs. These intensively examined and sampled boulders are inferred to be representative of the outcrops and boulders that abound on the upper massif slopes. Boulder tracks and distributions of boulders on the massifs suggest that the station 2 boulders came from the upper third of the South Massif and the station 6 boulder from about one-third of the way up the North Massif. There is no strong suggestive evidence to indicate the source area on. the North Massif for the station 7 boulder.

The boulder samples from all three stations as well as rock 73215 from the light mantle at station 3 have been studied intensively by teams of petrologists, geochemists, and geochronologists. Details are summarized in this report in the appropriate station and sample discussions. In general, the boulders are dominantly similar polymict breccia that consists of mineral and lithic clasts intimately mixed with a very fine coherent crystalline groundmass.

Directly observed and sampled lithic clasts range from metaclastic fragments smaller than 1 mm in size to the approximately 0.5x1.5 m clast of norite cataclasite in the station 7 boulder. The larger clasts are derivatives of the plutonic dunite-anorthosite-noritetroctolite suite; all have undergone thermal metamorphism or cataclasis before or during incorporation

in the enclosing breccia; some have undergone later local cataclasis. Mineral clasts, generally with little if any evidence of shock metamorphism, are mainly plagioclase, pyroxene, and olivine.

There is general agreement that the breccia matrices are laden with fragments, but the petrography and origin of the crystalline groundmasses are controversial. The consortium for boulder 1 at station 2 concluded that the competent breccia of boulder 1 was thermally metamorphosed and partly melted (Ryder and others, 1975). In contrast, the consortia investigating boulders 2 and 3 at station 2, sample 73215 from station 3, and the station 6 and 7 boulders interpreted the breccia matrix to have formed from a mechanical mixture of relatively cold unshocked fragmental debris and impact-generated silicate melt. In their views the melt, charged with lithic and mineral clasts, crystallized to subophitic to poikilitic texture with no evidence of recrystallization due to thermal metamorphism (Dymek and others, 1976b; James and Blanchard, 1976; Simonds, 1975; Chao and others, 1974; Chao and others, 1975a). However, some isolated rocks (for example, 76055) that resemble elements in the matrix of the station 6 boulder are inferred to have been thermally metamorphosed and contain clasts with poikilitic texture also interpreted as products of thermal metamorphism (Chao, 1973).

As the process of impact pulverization, heating, and melting yields a continuum of products, and as these may be thoroughly intermixed in the depositional process, the extent to which the final lithic product represents crystallization of a melt or recrystallization of heated rock powder intermixed with melt seems more an academic question than a substantive distinction. For example, the extremes of thermally metamorphosed and crystallized melt components of the matrix yield the same age for the event that formed them.

Microprobe data indicate that the crystalline groundmass in boulders 2 and 3 from station 2 is lower in $A1_20_3$ and MgO (Dymek and others, 1976b) and that the groundmass in sample 73215 is lower in $A1_20_3$ and CaO (James and Blanchard, 1976) than is the bulk breccia. Those workers concluded that the crystalline matrix could not have originated solely by crushing or melting of parent material of the composition of the clast assemblage.

However, it should be noted that the process of cataclastic breakdown of the plutonic rocks commonly pulverized the mafic minerals more than the plagioclase and concentrated the mafic components in the breccia matrix, a process also observed in cataclastic products of terrestrial impact structures (Wilshire, 1971). On the other hand, the character of plutonic rocks in the returned samples indicates that before impact the crustal rocks were layered and had widely divergent bulk compositions over short vertical distances (Jackson and others, 1975); the chances of mixing compositionally distinct layers during impact would be good.

Dymek and others (1976b) found that the dominant clastic plagioclase is more calcic than the groundmass plagioclase and that clastic olivine and pyroxene tend to be more magnesian than their groundmass counterparts in boulders 2 and 3. These relations are compatible with the hypothesis that the more refractory materials of the target tend to remain as clasts; the less refractory materials contribute preferentially to the melt.

Simonds (1975) found in the station 6 boulder that with increasing grain size of the groundmass, clast abundance and the ratios of mafic to feldspathic clasts and of pyroxene to olivine clasts decrease, whereas groundmass pyroxene and plagioclase become, respectively, more magnesian and more calcic. He related these systematic variations to the effect on cooling of the melt of the initial ratio of clasts to melt. Where

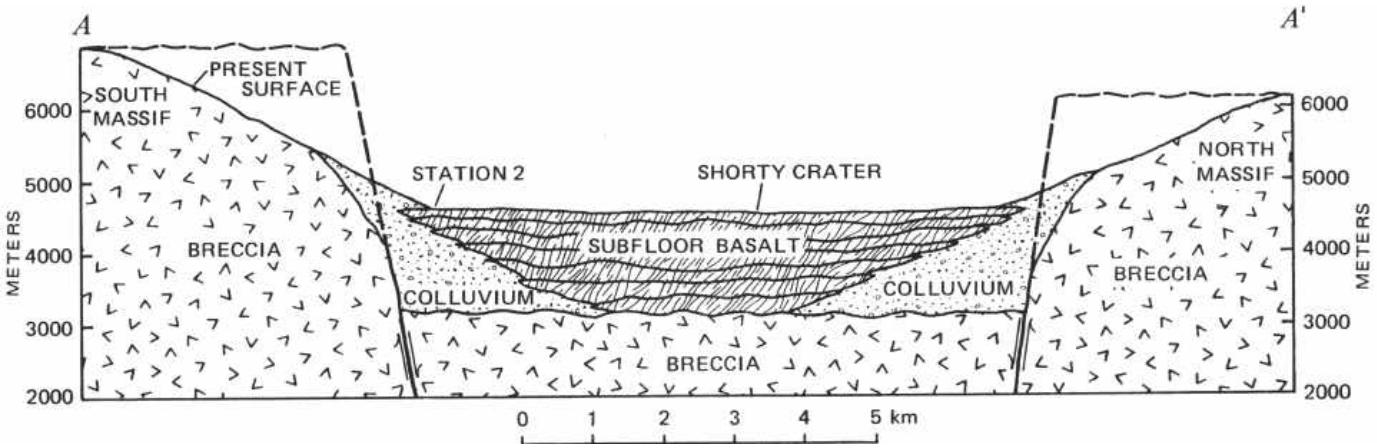

FIGURE 242.-Relations inferred among major subregolith units. Figure 6 shows line of section. Topographic profile derived from National Aeronautics and Space Administration 1:50,000-scale Lunar Topographic Map- Taurus-Littrow (1972). No vertical exaggeration. (From Wolfe and others, 1975.)

this ratio was high, the matrix was rapidly quenched; its grain size is extremely fine, and little or no digestion of clasts occurred. Where the ratio was lower, the melt was less rapidly quenched; hence, its grain size is coarser, and its composition was modified by digestion of the smaller and less refractory clasts.

In spite of these suggestions that the breccia formed by mixing of clasts and melt, the distinction between thermal metamorphic and melt origins for the crystalline groundmass is uncertain. The difficulty in petrologic interpretation is highlighted by the conclusion of James (1976b) that the sample 73215 aphanite, in her view an aggregate of clasts and impact melt, is equivalent in petrography and genesis to the competent breccia of boulder 1, which Ryder and others (1975) interpreted as high-grade metamorphic and partially melted. Chao and others (1975a) interpreted rims formed on xenocrysts in sample 77115 from the station 7 boulder as due to reaction during slow cooling of the enclosing melt. In the same paper, Huebner wrote a rebuttal arguing that the xenocryst rims resulted from subsolidus reaction with the matrix rather than from reaction with a melt (see discussion of sample 77115 for more detailed information). In addition, the compositional and textural relations reported by Simonds (1975) for the groundmass of the station 6 boulder samples could have resulted from progressing reaction between clasts and hot, fine-grained particulate matrix during thermal metamorphism.

In boulder 1 from station 2 and in samples 73215 and 73235 from station 3, the coherent crystalline breccia occurs as clasts in or is invaded by friable breccia or cataclasite. The Marble Cake clast in sample 72275 and the large clast in sample 72235 have cores of feldspathic cataclasite, partly fused in 72235, crudely interlayered and rimmed by crystalline polymict breccia. Polymict breccia and cataclasite are mutually interpenetrative; in the clast from sample 72235 the dark breccia coating is continuous with parts of the banded core. In these clasts both components, polymict breccia and feldspathic cataclasite, were undergoing cataclastic flow simultaneously (Ryder and others, 1975; Wilshire and Moore, 1974).

In sample 76255 from the station 6 boulder, fragments of coherent polymict breccia occur as clasts in norite cataclasite. Relations in the boulder and detailed petrographic study (Warner and others, 1976) show that the norite cataclasite is, in turn, a clast within coherent crystallized polymict breccia.

We infer that such intimate mixing of coherent crystalline breccia and friable breccia or cataclasite occurs not only at centimeter and meter scales, as seen in hand samples and boulders, but is characteristic in the Taurus-Littrow massifs at scales of tens and hundreds of meters. A telephoto view shows that the upper part of the South Massif (fig. 243) consists of irregular and discontinuous light and dark patches. Boulders are more highly concentrated in the dark patches, which suggests that the dark patches are underlain by more coherent material than the light patches.

Schmitt (1973) reported seeing, high on the South Massif, a linear color boundary with an apparent dip of 10° to 15° W. He suggested that blue-gray material below the boundary and tan-gray material above the boundary may have been represented in separate boulders sampled at the base of the massif. Close examination of orbital and surface photographs shows that this color boundary (fig. 243) may result from fortuitous alinement of some of the light patches. We agree that lithologic differences exist in the massif but suggest that the lithologic units occur in discontinuous pods or lenses rather than as subhorizontal continuous strata. By extrapolation from the intimate intermixture of coherent crystalline breccia, friable breccia, and cataclasite in the sampled boulders, we suggest that the discontinuous lenses seen in the massifs represent the same three rock types. The boulders themselves represent a sample biased toward the more coherent crystalline breccia.

Major-element data, summarized in figure 244, show, that the matrices of breccias from the massifs occupy a limited compositional range in which $A1_20_3$ values are approximately 16 to 23 percent. The major deviation from a well-defined narrow linear trend is shown in samples from rock 72275, which are deflected from the major trend toward the pigeonite basalt that occurs in the sample as clasts and as stringers of cataclasite (compare fig. 75). The matrices of the massif breccias, both competent and friable, are broadly noritic in composition. Rhodes and others (1974) recognized rocks in this compositional range as a major massif component, which they called noritic breccia.

A smaller group of analyzed samples is clustered at values of Al_20_3 of approximately 25 to 28 percent along the same linear trend (fig. 244). These are feldspathic plutonic or metaplutonic rocks-troctolite, gabbro, olivine norite, or their crushed or thermally metamorphosed equivalents-that occur as clasts in the breccia or were collected as loose rocks. Rhodes and others (1974) recognized this group as a second major massif component, which they called anorthositic gabbro on the basis of chemical composition.

An analyzed clast from sample 72255, boulder 1, station 2, extends the linear trend to the composition of anorthosite (A1203 greater than 35 percent). Sample 77215, the large norite cataclasite from the station 7

boulder, and the Civet Cat norite clast from sample 72255, boulder 1, station 2, extend the linear trend in the opposite direction to Al_2O_3 values of 14 to 16 percent (fig. 244). Norite samples (78235 and 78527) from the Sculptured Hills have intermediate compositions that are similar but not identical to the breccia matrices.

Major-element data for the regolith samples, summarized in figures 245 and 246, indicate that the highlands component of the regolith can be interpreted as a mixture of comminuted debris derived from breccia matrix material (approximately 16-23 percent $A1_20_3$, fig. 244) and feldspathic plutonic and metaplutonic rock (approximately 25-28 percent Al_2O_3, fig. 244). The more feldspathic component occurs as clasts within the breccia; presumably it also occurs within the lenses and stringers of friable cataclasite that we believe are a significant part of the massif rocks.

Rhodes and others (1974) gave "prevalent" compositions, plotted in figures 245 and 246, for the two massif components that they called noritic breccia and anorthositic gabbro. The compositions fit the data of figure 244 well at Al_20_3 values of approximately 18.0 and 26.5 percent; hence the joint between them in figures 245 and 246 reasonably represents the linear trends of figure 244. The highlands-regolith and light-mantle compositions (figs. 245 and 246) show a broad linear trend due to admixture of basalt and ash debris with highlands material. Data points for samples from stations 2 , 2a, and 3, where basalt and ash components are minimal or absent, lie on or near the noritic breccia-anorthositic gabbro join. Their positions along the join suggest that the breccia matrix component (noritic breccia of Rhodes and others) is significantly more abundant than the more feldspathic component (anorthositic gabbro of Rhodes and others). In contrast, Rhodes and others (1974) interpreted chemical data from the sediment samples as indicating general predominance of their anorthositic gabbro component. In either case, the sediment composition may not truly represent the bulk massif composition. It suggests, however, that relatively feldspathic material (Al_2O_3 greater than about 25 percent) is more voluminous than might be inferred from its frequency in the massif' rock samples.

The massif samples represent rocks from different parts of the two massifs. Those from station 2 probably carne from about 1,500 m above the valley floor. The massif breccia at station 3, in the light mantle, came from regolith material transported from an unknown area, perhaps the upper part, of the South Massif. The station 6 houlder apparently rolled from about 500 m above the valley floor on the North Massif, and the source of the station 7 boulder on the North Massif is unknown.

These samples are strikingly uniform in petrographic character and in chemical composition. The only significant deviation from the very narrow range in major-element compositions of the breccia matrix is probably due to local admixture of the pigeonite basalt debris of sample 72275 (figs. 75, 244). Winzer and others (l975a) , summarizing large-ion lithophile element data for boulder 1 from station 2, sample 73215, and the stations 6 and 7 boulders, concluded that all are so closely similar as to be considered identical.

Morgan and others (1975) found that most of the Apollo 17 massif breccia shows a distinctive meteoritic trace-element distribution (their group 2) that they believe represents the trace-element signature of the projectile that impacted to form the Serenitatis basin (southern Serenitatis basin of this report). Samples from boulder 1 have a distinctively different trace

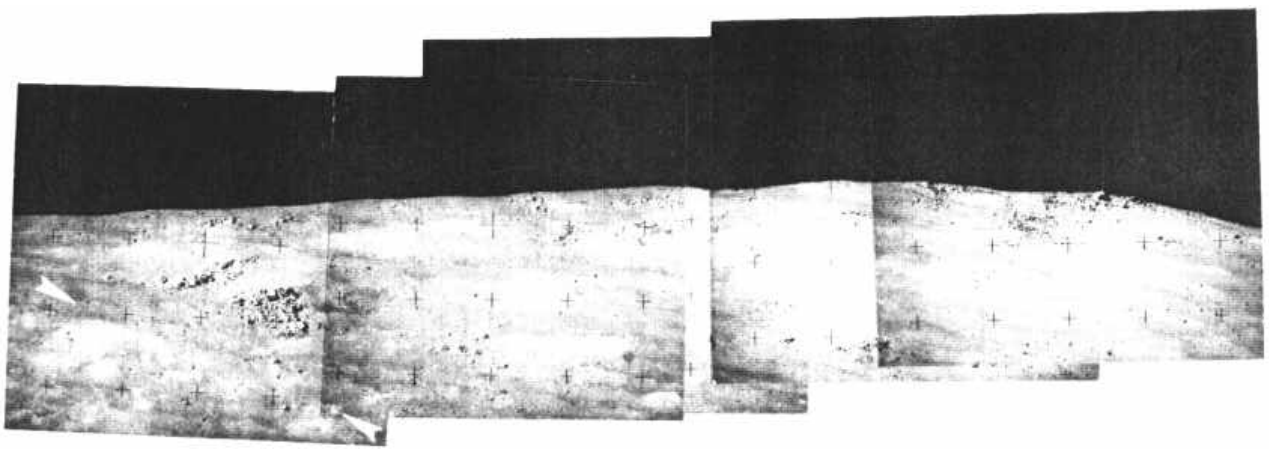

FIGURE 243.- Telephoto panorama showing light-colored and bouldery patches on South Massif. Large patch of boulders at left may be source of station 2 boulders. Arrows are approximately alined with color boundary described by Schmitt (1973). Width of view is approximately 6 km. (NASA photog-raphsAS17-144-22051-22057.) (From Reed and Wolfe, 1975.)

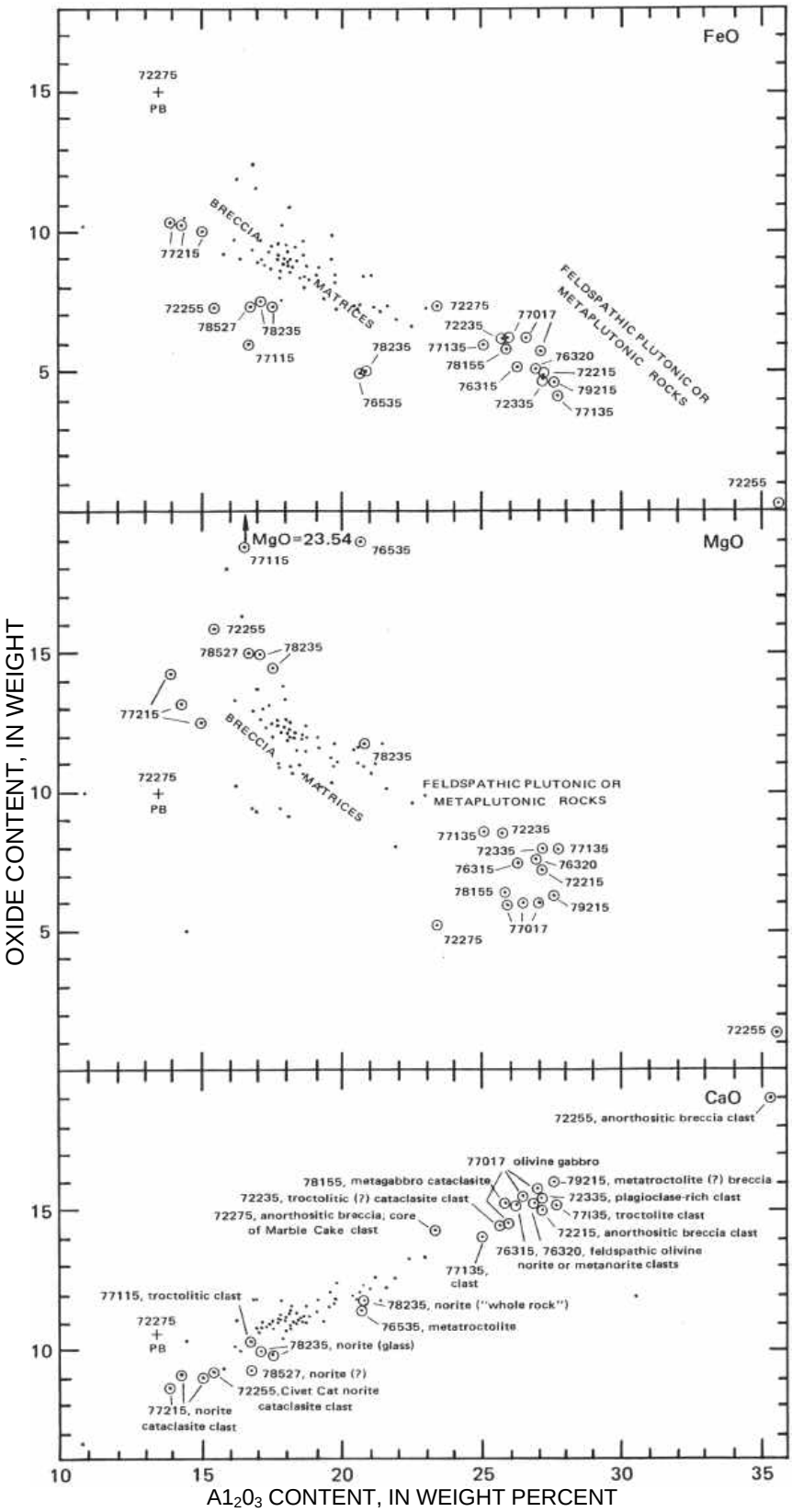

FIGURE 244.-Summary plots of FeO, MgO, and CaO contents in relation to $A1_20_3$ content for all analyzed Apollo 17 highlands rocks. See sample descriptions for analyses and sources of data. Dots, matrix or presumed matrix of massif breccia; circled dots, plutonic or metaplutonic rocks of the massifs and Sculptured Hills; +PB, pigeonite basalt of sample 72275.

element pattern (their group 3). However, trace element patterns of groups 2 and 3 have been identified from about a centimeter apart within apparently identical matrix material in sample 73215 (James and others, 1975a). Hence, the two distinct trace-element distributions apparently occur within the same basin ejecta unit.

We conclude from the narrow range of rock types, textures, and major- and trace-element compositions that samples from widely differing parts of the two massifs are virtually identical rocks derived from a single grossly homogeneous ejecta unit represented by at least the exposed portions of the massifs. In detail, the ejecta unit is heterogeneous. It consists of complexly intermixed pods or lenses of coherent polymict breccia, friable polymict breccia, and cataclasite formed from crushed plutonic or metaplutonic rock.

During the southern Serenitatis impact, target material was fractured, sheared, crushed, or melted depending upon its location with respect to the wall of the rapidly expanding transient cavity. Crushed rock and melt, mobilized and violently mixed, moved upward along the margins of the growing crater with the shearing motion of cataclastic flow (Wilshire and Moore, 1974). This shearing effect is recorded in such fabrics as the lamination of boulder 1 from station 2, the crude interlayering of feldspathic cataclasite and dark competent breccia in some of the clasts of boulder 1, lithologic banding and development of schlieren in sample 73215, and the occurrence in the station 7 boulder of vesicles in green-gray breccia that are both elongated and alined in trains parallel to the contact with the enveloped blue-gray breccia.

Mobilization and cataclastic flow mixed relatively cold, unshocked mineral and lithic debris with hot, pulverized to molten rock. Extreme temperature gradients existed through short distances. At millimeter and submillimeter scales, thermal equilibrium between superheated melt and cold clasts was largely achieved within seconds (Simonds, 1975; Onorato and others,

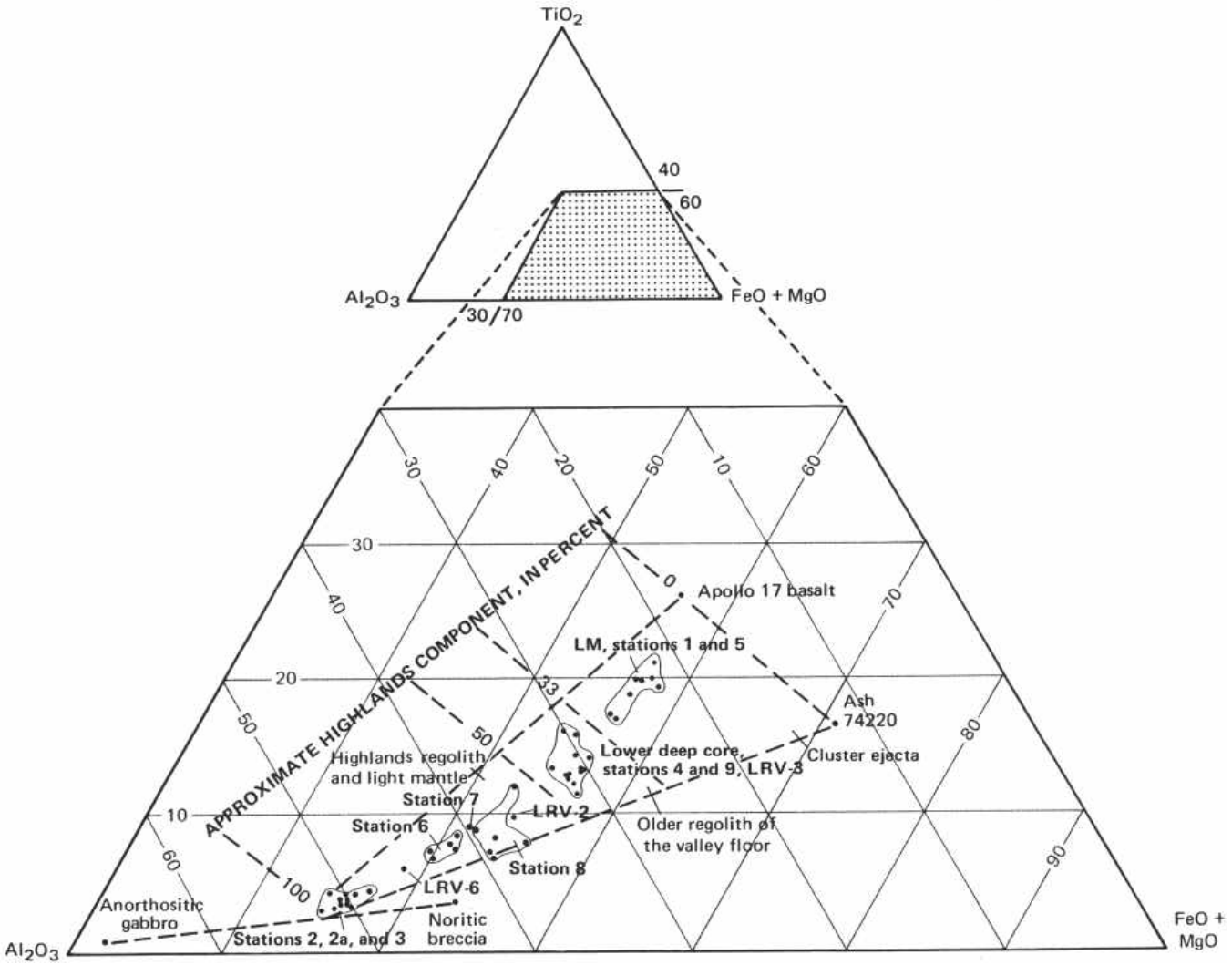

FIGURE 245.-Relative amounts of $Ti0_2$, Al_20_3, and FeO+MgO in sediment samples grouped by station and stratigraphic unit. Compare with figure 246. Apollo 17 basalt, anorthositic gabbro, and noritic breccia values from Rhodes and others (1974). See sample descriptions for analyses and sources of data for sediment samples.

1976). Where quenching times were sufficiently long, small and less refractory clasts were preferentially digested by the melt; the surviving clasts tend to be biased toward the more refractory compositions (Simonds, 1975). In addition, finely particulate groundmass material may have been biased toward more mafic composition because of preferential concentration in the groundmass of the more easily crushed mafic minerals. These factors may account for the slight differences between crystalline groundmass compositions and bulk breccia matrix compositions reported by Dymek and others (1976b) and by James and Blanchard (1976). On a larger scale, quenched melt fractions were themselves disrupted and. mixed with continuously disrupted solid debris during ejection. This produced rocks such as boulder 1, station 2, that contain clasts of the same dark microbreccia as forms the matrix of the coherent breccia.

Immediately after deposition, the ejecta deposit was thermally heterogeneous at scales from centimeters to tens or hundreds of meters. Hot fragmental to partly molten ejecta and relatively cool cataclasite and coherent lithic clasts were intermixed in a melange of lenses, pods, and veins. In this environment, crystallization of the breccia matrix may have resulted both from cooling of the partial melts and from thermal metamorphism of fine-grained materials. Because of the large thermal heterogeneities, the final matrix ranges over short distances from friable to granoblastic or poikilitic and impact fused.

The massif boulders show breccia-within-breccia. Clasts of breccia have been interpreted as recording impact events before the one that created the apparently youngest matrix, and they have led to the conclusion that the target material was largely preexisting breccia (for example, Ryder and others, 1975; Wolfe

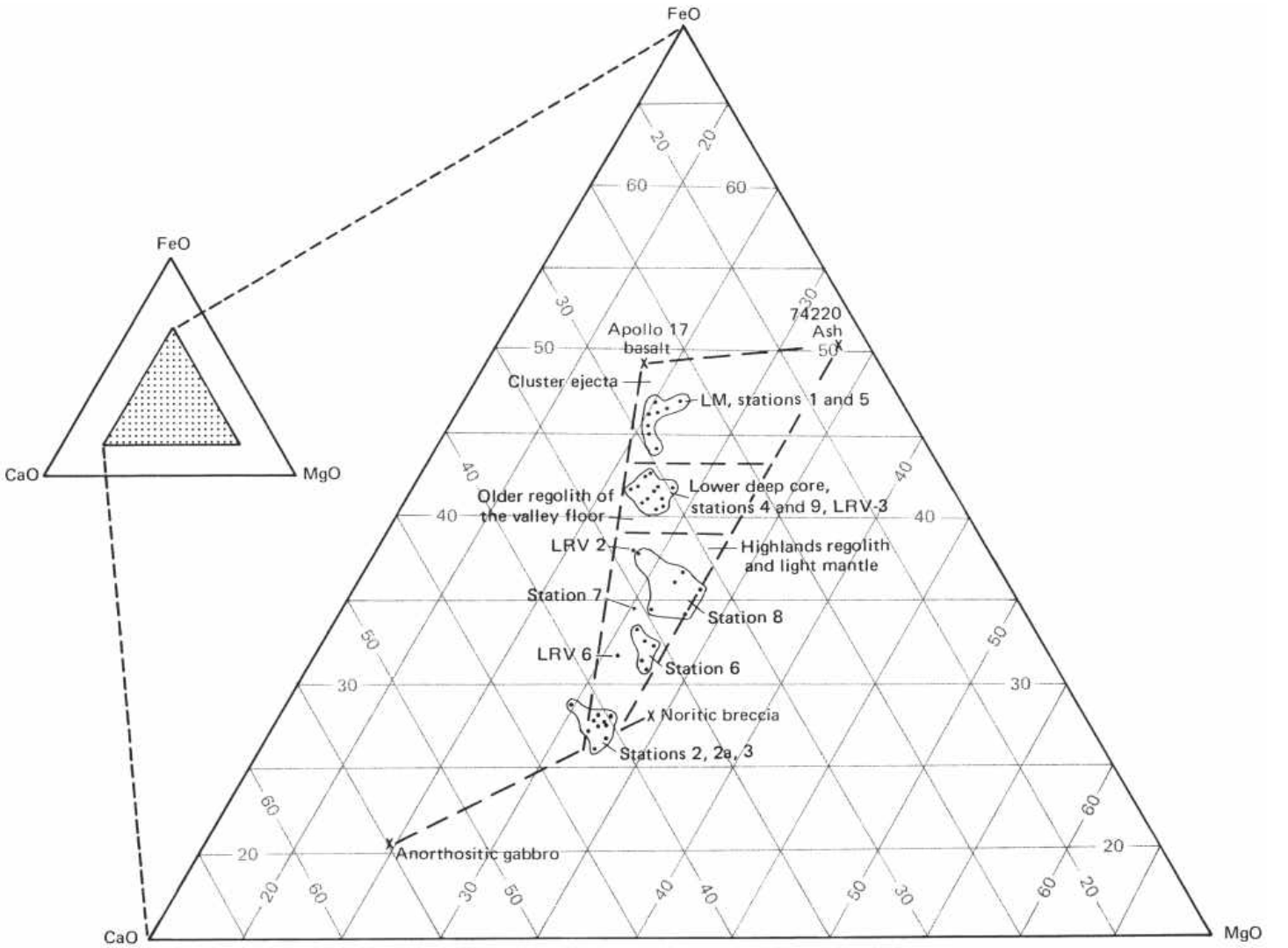

FIGURE 246.-Relative amounts of FeO, CaO, and MgO in sediment samples grouped by station and stratigraphic unit. Compare with figure 245. Apollo 17 basalt, anorthositic gabbro, and noritic breccia values from Rhodes and others (1974). See sample descriptions for analyses and sources of data for sediment samples.

and Reed, 1976). However, in the thermally heterogeneous ejecta deposit that we postulate, friable and competent crystalline breccia in juxtaposition can be interpreted as products of the same impact event rather than of multiple impacts. Hence, clasts of breccia and the matrix that encloses them are commonly similar in composition. For example, the competent breccia rind of the Marble Cake clast in sample 72275 shows the same distinctive relative enrichment in FeO and CaO and relative depletion in MgO with respect to $A1_20_3$ (fig. 75) that characterizes the enclosing friable matrix.

The station 7 boulder provides evidence that clasts of aggregated ejecta may develop and maintain coherence during transport and deposition of the ejecta. Fractured blue-gray breccia is enclosed in a matrix of relatively unfractured vesicular greenish-gray breccia (figs. 180 and 185). Vesicles in the apparently younger greenish-gray breccia are flattened and alined in trains parallel to the contact. The apparently older blue-gray breccia envelops and intrudes a large fragile clast of norite cataclasite (sample 77215). The matrices of the two breccias are nearly identical in composition (fig. 179) and have more or less similar finely crystalline texture. In agreement with Winzer and others (1977), we believe that their similar compositions and textures are unlikely to have resulted from separate impact events. In addition, the apparently older breccia, with its fragile clast, shows no evidence of the cataclasis that might be expected had it been target material that was crushed and melted to form the apparently younger breccia. Hence, we postulate that the bluegray breccia aggregated and developed sufficient coherence during transport of the ejecta to develop and maintain fractures while being enclosed in still highly mobile cogenetic ejecta.

In accord with the postulate that breccia-within-breccia fabric may form in single impact events, we suggest that the material that was crushed and melted to create the massif breccia was largely excavated for the first time by the southern Serenitatis impact. The population. of clasts of identifiable plutonic parentage indicates that the target was a plutonic complex that included dunite, norite, troctolite, gabbro, and anorthosite. Textural evidence from some of the samples (for example, metadunite 72415-18 and metatroctolite 76535) shows that some of the plutonic target rocks had undergone a prolonged deep-seated thermal metamorphism, the Apollonian metamorphism of Stewart (1975), before their excavation by the southern Serenitatis impact.

The linear compositional trends of the breccia matrix (fig. 244) may represent a mixing line. The dominant end members may have been (1) crushed or melted norite broadly like the norite cataclasite of sample 77215 and the Civet Cat clast in sample 72255 and (2) crushed or melted rock derived from the more feldspathic plutonic rocks (approximately 25 to 28 percent $A1_20_3$, fig. 244). Parent rocks of more extreme composition (for example, metadunite 72415-18, metatroctolite 76535, and anorthosite like the highly aluminous clast from sample 72255) were minor components. Winzer and others (1977) reached similar conclusions.

Plutonic rocks with a compositional range much like that of the southern Serenitatis target rocks occur together in relatively small plutonic bodies in the Earth's crust. Hence, no part of the suite is necessarily a sample of lunar mantle.

Chromian spinel-bronzite-diopside symplectites in metatroctolite 76535 may have formed during slow crystallization of a pluton at a 10-30-km depth (Gooley and others, 1974). Because of the uncertainties involved, Dymek and others (1975) objected to this specific depth calculation, but they agreed that. the rock had crystallized at fairly great depth. Stewart (1975) inferred from the granular-polygonal texture that the sample had been annealed on the order of 10' years at a depth of 7 km or more.

Spinel cataclasites from samples collected at stations 2, 3, and 6 have the mineral assemblage anorthositealuminous enstatite-olivine-spinel. If this is an equilibrium assemblage, it may have crystallized at pressures of about 3 to 7.5 kb, equivalent to lunar depths of about 60 to 150 km. The small amount of iron in the assemblages may reduce the estimated pressure, but estimated depths are consistent with derivation from the lower crust (Bence and others, 1974; Bence and McGee, 1976).

Approximately 90 radiometric age determinations for Apollo 17 highlands rocks are summarized graphically in figure 247. If, as we believe, these rocks are samples of ejecta from the southern Serenitatis basin, their radiometric ages may date the impact. However, interpretation is complicated because the radiogenic clocks of the target materials were not uniformly reset. Many rocks contain relict grains of the original plutonic assemblage that retain to various degrees their crystallization ages. Others retain a preexcavation metamorphic overprint, and some may have been modified by smaller, more recent impacts.

Several samples clearly record events older than the southern Serenitatis impact. Partly metamorphosed dunite 72417, from boulder 3 at station 2, and troctolite 76535 have Rb-Sr isochron ages, respectively, of 4.55 and 4.61 b.y. These have been interpreted as primary crystallization ages (Papanastassiou and Wasserburg, 1975, 1976). Ages near 4.25 b.y. have also been

determined for metatroctolite 76535 by other techniques. Papanastassiou and Wasserburg (1976)

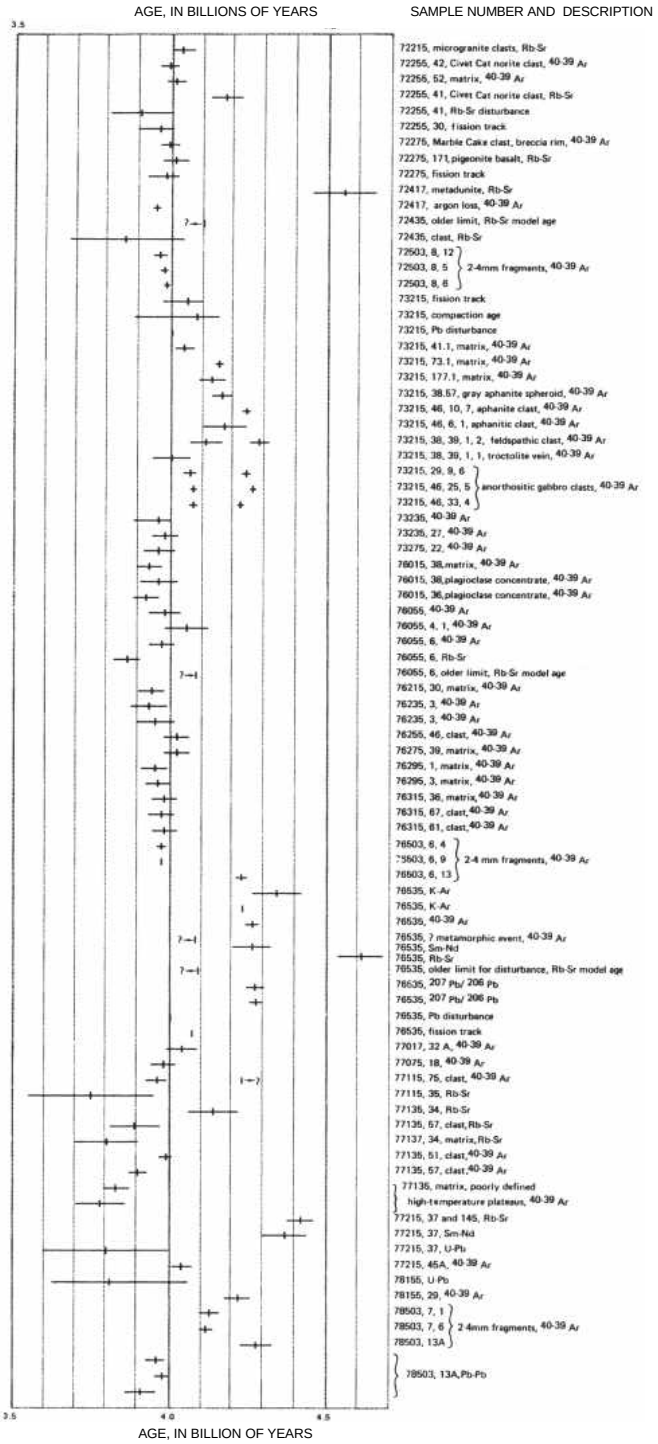

FIGURE 247.-Graphic summary of published radiometric ages for Apollo 17 highlands rock samples. See individual sample discussions for sources of data.

suggested that the temperature of the parent troctolite body remained sufficently high until approximately 4.25 b.y. ago to permit degassing of Ar and chemical and isotopic exchange of Sm and Nd. Rb-Sr systems, equilibrated 4.61 b.y. ago when the rock initially crystallized, were protected from exchange by impervious.enclosing olivine. The proposed episode of elevated temperature could have been responsible for the deepseated thermal metamorphism that recrystallized both the troctolite and the dunite (Apollonian metamorphism of Stewart, 1975).

Other rocks whose radiometric ages record distinct presouthern Serenitatis events include the Civet Cat norite clast from boulder 1 at station 2, 4.17 b.y. (Compston and others, 1975); clasts in sample 73215 from station 3, approximately 4.25 b.y. (Jessberger and others, 1976b); norite cataclasite clast 77215 from the station 7 boulder, approximately 4.4 b.y. (Nakamura and others, 1976); and some 2-4-mm fragments, 4.13-4.28 b.y. (Schaeffer and others, 1976; Schaeffer and Husain, 1974; Kirsten and Horn, 1974). These ages are younger limits for primary crystallization or for older metamorphic events, because some isotopic equilibration or degassing of argon may have occurred in the southern Serenitatis impact.

Some plutonic or metaplutonic fragments in the ejecta apparently had their radiogenic clocks completely reset. For example, sample 76235, olivine metanorite cataclasite from a large clast in the station 6 boulder, gave $^{40-39}$Ar ages of 3.93 and 3.95 b.y. (Cadogan and Turner, 1976). These are equivalent to the ages determined for the enclosing breccia (fig. 247). Cadogan and Turner (1976) inferred that the clast was strongly heated, resulting in complete degassing of argon during the impact that assembled the materials of the station 6 boulder.

The majority of radiometric ages for massif breccia were determined by the $^{40-39}$Ar technique. Except for two dates for sample 77135 that were determined from short, poorly defined, high-temperature plateaus (Stettler and others, 1974), the $^{40-39}$Ar ages range from 3.90 to 4.24 b.y. and are strongly clustered between approximately 3.9 and 4.0 b.y. (fig. 247).

All of the $^{40-39}$Ar breccia ages greater than 4.05 b.y. are from sample 73215. Evaluating their results for 73215, Jessberger and others (1976b) considered an age of approximately 4.05 b.y. as an older limit for the event that formed the aphanitic breccia matrix, because the abundant small clasts were presumably incompletely outgassed.

If outgassing of argon ranged from partial to complete or nearly complete in the southern Serenitatis ejecta, the measured ages may approach or reach a lower limit that is equivalent to the age of the southern

Serenitatis impact. The concentration of $^{40-39Ar}$ ages between 3.9 and 4.0 b.y. may represent that limit, which is in agreement with the conclusion of Cadogan and Turner (1976) that the materials of the station 6 boulder were assembled 3.96±0.04 b.y. ago. Rb-Sr ages for clasts of microgranite and pigeonite basalt, respectively 4.03 and 4.01 b.y. (Compston and others, 1975) , impose older limits on the assembly of boulder 1 that are compatible with the overall $^{40-39}$Ar results.

Six Rb-Sr ages of breccia or of clasts within breccia and one U-Pb age (clast in 77215) are in the range from 3.75 to 3.90 b.y. Except for the 3.86±0.04-b.y. age for breccia 76055 (Tera and others, 1974b) , published analytical errors for these ages are sufficiently large to overlap the 3.9 to 4.0 b.y. concentration of $^{40-39}$Ar ages (fig. 247).

For three of these samples (77115,35; 77137,34; 77215,37) the mean ages, 3.75-3.80 b.y. (Nakamura and others, 1976; Nunes and others, 1976; Nunes and others, 1974), are within the range of mean ages determined by both Rb-Sr and $^{40-39}$Ar techniques for subfloor basalt samples. Photogeologic and field evidence indicate that the massif materials are older than the sampled part of the subfloor basalt. Hence, these younger ages (</=3.80 b.y.) for massif materials do not date the age of breccia formation.

The other four young Rb-Sr ages are (1) an estimate of 3.90±0.1 b.y. for a Rb-Sr disturbance recorded in Civet Cat norite clast 72255,41 (Compston and others, 1974), (2) a Rb-Sr isochron age of 3.85±0.18 b.y. for a clast in sample 72435 (Papanastassiou and Wasserburg, 1975) , (3) a two-point Rb-Sr isochron age of 3.86±0.04 b.y. for metamorphosed breccia 76055 (Tera and others, 1974b), and (4) a Rb-Sr isochron age of 3.89±0.08 b.y. (Nunes and others, 1974) for a clast, sample 77135,57, which also gave a $^{40-39}$Ar age of 3.90±0.03 b.y. (Stettler and others, 1975). At best, these data may suggest that the 3.9 to 4.0 b.y. cluster of $^{40-39}$Ar ages could be slightly older than the true age of the southern Serenitatis impact, perhaps because of argon entrapment.

SCULPTURED HILLS

As already described, material of the Sculptured Hills, by analogy to the knobby facies of the Montes Rook Formation of the Orientale basin (Scott and others, 1977), is interpreted as ejecta of the southern Serenitatis basin. The unit was deposited after deposition and faulting of the massif breccia. The Sculptured Hills differ markedly from the massifs because of their distinctive hummocky topographic form, undulating gentler slopes, absence of resistant ledges, and near absence of boulders.

Orbital and lunar surface photographs show that station 8 is in an area of dark, relatively fine surficial material. Regolith samples contain a large admixture of valley-floor material, probably dominantly ash (figs. 245 and 246). Rock fragments are mainly basalt and regolith breccia. Apparently the station 8 area is largely mantled by ejecta from the valley floor and by volcanic ash. Hence, we do not have a definitive sample of Sculptured Hills material.

No crystalline breccia was seen by the crew or included among the larger samples. Three fragments that might represent crystalline breccia matrix material were found among the 27 fragments of 2-4-mm size that were examined in sample 78503 (Bence and others, 1974). The other 24 fragments were identified as basalt (14) , regolith breccia (5) , glass (2) , and anorthosite-norite-troctolite (3).

Three highland rocks weighing more than 5 g were sampled. These are metagabbro cataclasite (78155), norite boulder (78235-38 , 78255) , and a noritic rakesample fragment (78527) . Any or all of these could have been transported from outside the Sculptured Hills to the station 8 area by impacts younger than the southern Serenitatis basin event. However, if they are Sculptured Hills fragments and if competent massiftype breccia really is scarce or absent as suggested by its absence in the samples, by the scarcity of boulders and ledges, and by the hummocky subdued topographic form of the Sculptured Hills, we can tentatively suggest that the Sculptured Hills unit is predominantly friable cataclasite excavated from the plutonic and metaplutonic rocks of the southern Serenitatis target.

HIGHLANDS MATERIALS YOUNGER THAN THE SOUTH ERN SERENI TATIS BASIN

Basin ejecta younger than the southern Serenitatis basin may occur in the Taurus-Littrow highlands. Moore and others (1974) have suggested that the Apollo 17 site lies within the area that may have been blanketed by Imbrium ejecta. Crisium ejecta might also be present in the Apollo 17 area. Scott and Pohn (1972) have mapped lineated terrain north of the crater Littrow as well as still farther north in the vicinity of the Taurus Mountains. They suggested that in the latter area the lineated terrain, which is radial to the Imbrium basin and was mapped by Wilhelms and McCauley (1971) as the Fra Mauro Formation, may include Imbrium ejecta. The lineated terrain north of Littrow, which was regarded as pre-Imbrium by Wilhelms and McCauley (1971), is not radial to either Imbrium or Crisium; we assume that it represents basin or large-crater ejecta deposited before the Imbrium impact. Scott and Pohn (1972) did not recognize any lineated terrain south of Littrow. The preservation of pre-Imbrium lineated terrain north of Littrow and the

absence of sculpturing related to Imbrium or Crisium in the Taurus-Littrow area suggest that Imbrium and Crisium ejecta, if present, are thin or scattered in the Taurus-Littrow area.

Further evidence that ejecta from Imbrium or Crisium is thin, scattered, or absent in the Apollo 17 area is provided by the preservation of the Sculptured Hills topography. If our correlation of the Littrow ring and the outer Rook ring is valid, the Sculptured Hills terrain is related in origin to the southern Serenitatis impact. Its distinctive topography would not be visible through great thicknesses of Imbrium and Crisium ejecta.

In addition to the physiographic evidence, the chemical and petrographic similarities of the massif breccia samples, particularly the boulders from stations 2, 6, and 7 and breccia samples 73215, 73235, and 73275 from station 3, strongly suggest that they represent ejecta from a single impact. There is no compelling evidence from the samples that ejecta from basins younger than southern Serenitatis has been sampled.

SUBFLOOR BASALT

Basalt, estimated to be about 1,400 m thick in the landing site (Cooper and others, 1974) , partially flooded the Taurus-Littrow graben. It rests on a surface that is presumably underlain by breccia near the axis of the valley and by the colluvial wedges near the valley margins (fig. 242). Because the informal name subfloor basalt has been used repeatedly for the basalt of the landing site since the time of the mission, we continue its use here. It is part of a regionally extensive unit designated Imb2 in plate 1.

The upper surface of the subfloor basalt is overlain by volcanic ash and impact-generated regolith with an estimated average combined thickness of 14 m (fig. 248). All sampled basalt was collected from the regolith.

Basalt fragments a centimeter or more in size were collected at all stations except 2 and 2a and some of the LRV stops. Basalt boulders half a meter or more in size were sampled in the LM area and at stations 1, 4, and 5. Boulders at stations 1, 4, and 5 may have been excavated for the first time from the subfloor basalt by the impacts that formed, respectively, Steno, Shorty, and Camelot craters. Smaller fragments and the boulders of the LM area (for example Geophone rock) cannot be related to specific source craters. Most are probably from the upper part, perhaps the upper 100 m or so, of the subfloor basalt.

On the basis of direct field observations, Schmitt (1973) described the basalt blocks in the central valley floor as "mostly massive, tan to pinkish gray coarsegrained ilmenite basalt having a generally coarsely ophitic and vesicular texture." Layering in the blocks at Camelot crater was recognized as due to differences in vesicle concentrations. Vugs and vesicles range from less than 1 percent to 30 percent by volume in the basalts, and their occurrence as layers is described in several of the station l rake samples (Butler, 1973).

The mineral proportions in the basalts vary widely. A compilation by Papike and others (1976) gives the following ranges (excluding one sample with 54 percent mesostasis): clinopyroxene 42-51 percent; olivine 0-10 percent; plagioclase 14-33 percent; opaque minerals (mainly ilmenite, armalcolite, spinel) 15-30 percent; silica (tridymite?) 0-5 percent. Textures range from very fine (grain size 0.25 mm or less) to coarse (grain size up to 2-3 mm).

The Apollo 17 basalt has been divided into two types on the basis of texture and mineralogy (Papike and others, 1974; Papike and others, 1976; Brown and others, 1975; Warner and others, 1975b). Most of the examined samples are in the very-high-titanium basalt group of Papike and others (1976). They include both fine- and coarse-grained olivine basalts that are broadly similar in major-element composition and that have been inferred to vary in grain size because of differences in cooling rates (Papike and others, 1974, 1976; Warner and others, 1975b).

The second type, Apollo 17 low-potassium basalt of Papike and others (1976) , resembles the Apollo 11 low-potassium basalt in texture and mineralogy. This basalt, characterized by scarcity or absence of olivine, is represented by the large blocks on the rim of Camelot crater (samples 75015, 75035, 75055) and by 5 out of more than 100 basaltic rake-sample and 2-4-mm fragments (Papike and others, 1974; Warner and others, 1975b) from widely separated parts of the traverse area.

The early published major-element chemical data suggested that the basalts formed two narrowly ranging and mutually exclusive compositional groups that coincided with the two petrographic groups. The olivine-poor basalts (Apollo 17 low-potassium type) were quartz normative; the dominant olivine basalts (very-high-titanium basalt) were olivine normative. Papike and others (1974) suggested that the abundant fine- and coarse-grained basalt of the latter type might be from, respectively, the rapidly cooled top and the slowly cooled center of a single lava flow. Subsequently, Papike and others (1976) concluded that the absence of a systematic correlation between majorelement composition and grain size may indicate that the very-high-titanium basalt samples came from multiple cooling units.

Considering the restricted occurence of the quartznormative basalt (Apollo 17 low-potassium type) on the

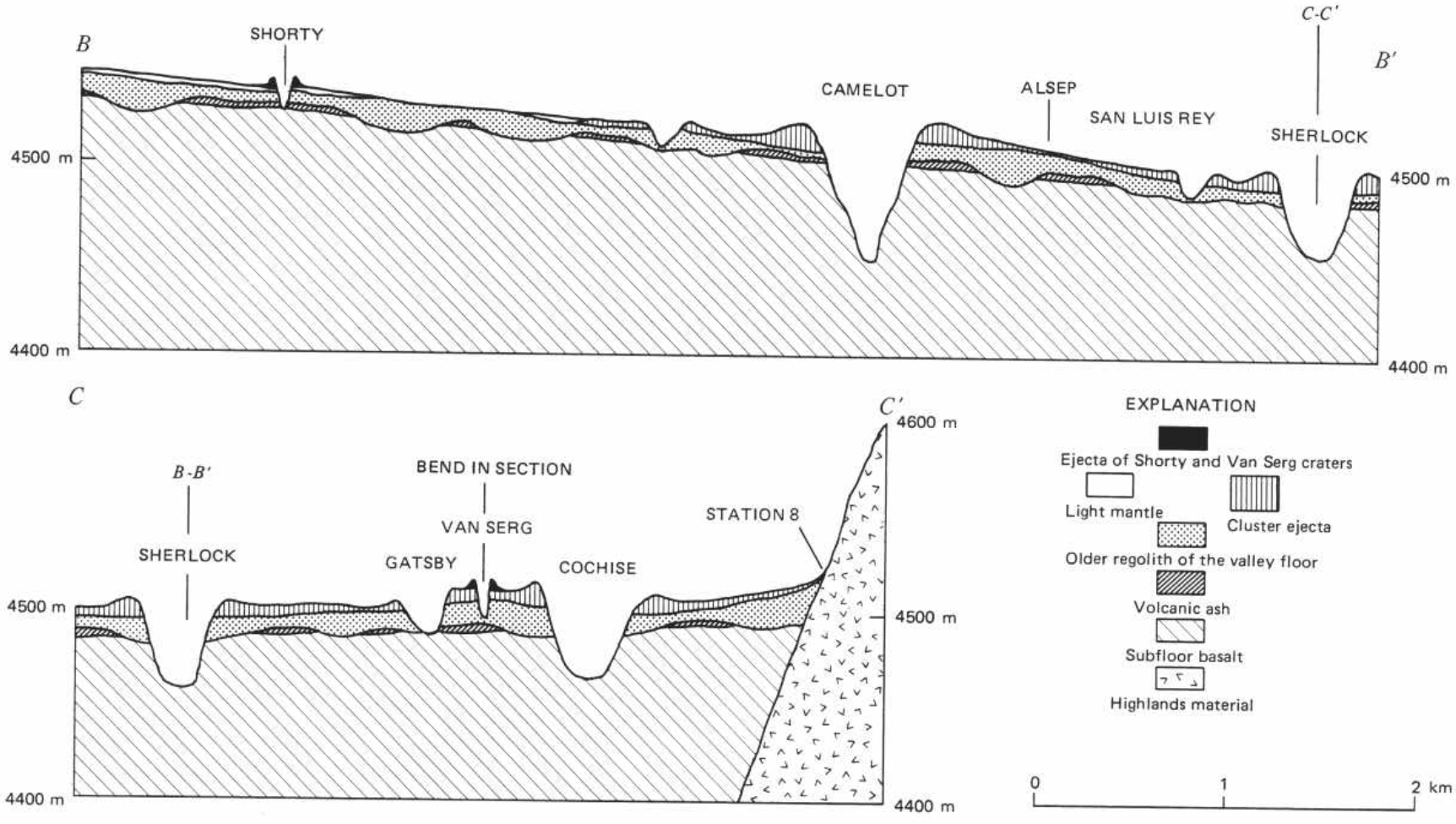

FIGURE 248.- Cross sections showing relations inferred among the subfloor basalt and the overlying volcanic ash and regolith units. Figure 6 shows locations of sections. Topographic profile derived from National Aeronautics and Space Administration 1:50,000-scale Lunar Topographic Map- Taurus-Liittrow (1972). Vertiical exaggeration is x 10. (Modified from Wolfe and others, 1975.)

Camelot crater rim and the ubiquity of the olivinenormative basalt (very-high-titanium basalt), Wolfe and others (1975) suggested that the olivine basalt, either as a single flow or as multiple flows of similar mineralogy and composition, might be about 100 m thick. Only the deepest crater, Camelot, was able to penetrate it and excavate the underlying quartznormative basalt.

More recent data favor a different model. The compositional gap between the two once-distinct types has been filled; the range of quartz-normative basalt extends to more mafic basalt than that identified as Apollo 17 low-potassium type (Rhodes and others, 1976). Trace-element data (Shih and others, 1975; Rhodes and others, 1976) led Rhodes and others (1976) to identify three basalt types, each derived from a separate chemically distinct parent magma. A number of samples cannot be consistently identified with one of the three types; these have been classed as basalt with uncertain affiliations. Each of the three types is characterized by distinctive trace-element distributions and ratios, particularly with respect to incompatible elements. For example, types A, B, and C are characterized respectively by mutually exclusive Ba/Rb ratios of approximately 140 to 160, 160 to 175, and 55 to 60 (Rhodes and others, 1976).

Applying low-pressure experimental data of Longhi and others (1974), Rhodes and others (1976) concluded that variations in major-element composition were due largely to near-surface crystal fractionation involving olivine, armalcolite and ilmenite, and chromian spinel. Increasing fractionation produced linear compositional trends characterized by increasing $Si0_2$, CaO, and $A1_20_3$ and by decreasing MgO, FeO, $Ti0_2$, and Cr_20_3- Silica variation diagrams (fig. 249) show these trends. MgO, CaO, and Cr_20_3 have been selected because they effectively separate the basalt types and show the similar differentiation trends of types A and B. Type C is characterized by FeO values as uniquely low with respect to other basalt as its MgO values are high. No highly fractionated members of type C have been identified.

Recognition of these compositional groups brings a degree of order to the otherwise scattered majorelement data. In this scheme, the so-called Apollo 17 low-potassium basalt (75015, 75035, and 75055) represents not a seperate lava type but a highly fractionated member of the type A basalt. These samples, from the rim of Camelot crater, are coarse grained; the extensive fractionation that they represent may have occurred during slow cooling of a relatively thick, deeply buried cooling unit (Rhodes and others, 1976).

Some tentative stratigraphic relations can be interpreted from the distribution of basalt samples with re-

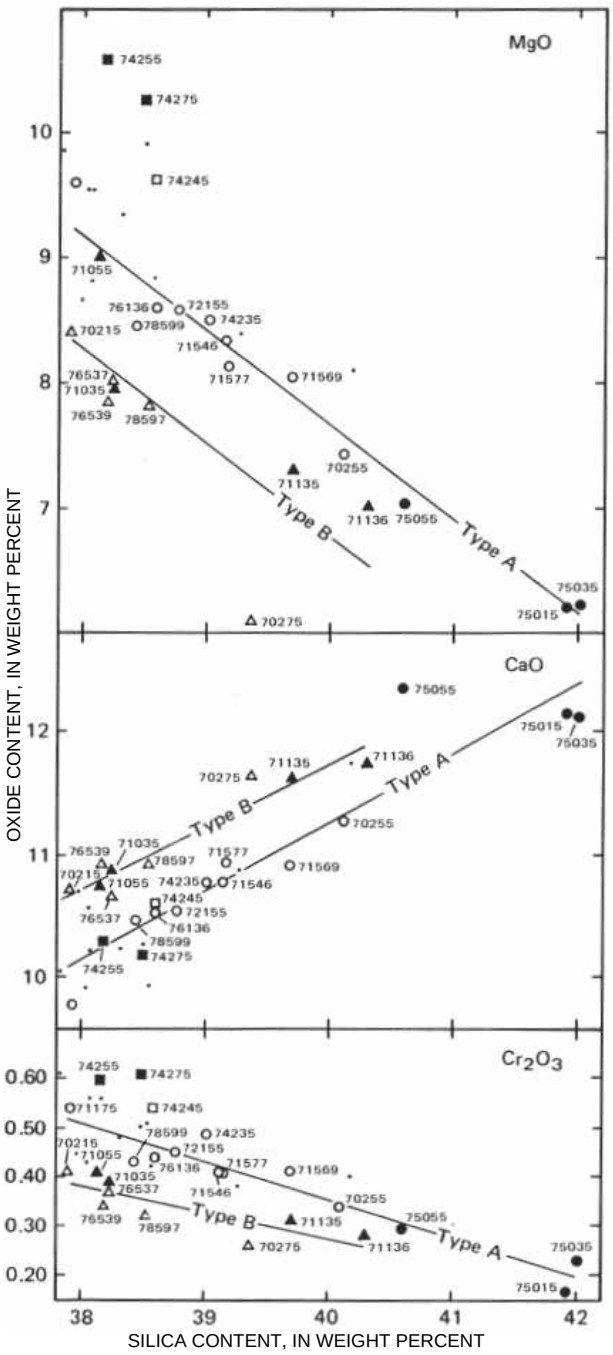

FIGURE 249.-Silica variation diagrams for Apollo 17 basalt. See sample descriptions for analyses and sources of data. Circles, triangles, squares, and dots represent, respectively, types A, B, and C, and basalt of uncertain affiliation of Rhodes and others (1976). Filled symbols represent boulder samples that are related to specific large craters. Best-fit lines are shown for types A and B. Samples 71055 and 75035 were not classified by Rhodes and others; 71055 is from same boulder as type-B sample 71035; 75035, from the rim of Camelot crater, has same major element chemistry and field occurrence as type-A sample 75055.

spect to Shorty, Steno, and Camelot craters. Type C basalt samples 74255 and 74275, came from, respectively, 5-m and 20-cm boulders on the rim of Shorty crater (fig. 120). Type C basalts have been identified at no other locality. Field and topographic evidence suggests that the Shorty impact excavated down to or just into the subfloor basalt. Hence, it is probable that the type C basalt represents the uppermost subfloor basalt in the vicinity of Shorty.

Type B basalt was collected at station 1 from two half-meter boulders on the rim of a fresh 10-m crater (figs. 35, 41) located 150 m from the rim crest of the 600-m Steno crater. It is likely that the impact that formed the 10-m crater reexcavated these boulders from the Steno crater ejecta, or at least repositioned them. Because the boulders are 150 m out on the Steno ejecta blanket, they probably came from an intermediate depth, perhaps some tens of meters, in the Steno target.

The highly fractionated type A basalt samples were collected from three large blocks on the rim of the 650-m crater Camelot (figs. 132, 135). Because they occur on the rim of the largest sampled crater, they may be from the deepest sampled part of the subfloor basalt. A depth of 100 m or more is possible.

The simplest interpretation of these relations is that at least three flow units, in ascending order, highly fractionated type A basalt, type B basalt, and type C basalt, are represented in the basalt samples. Whether types A, B, and C occur as single or multiple flow units and whether such multiple units are complexly interlayered with each other as well as with basalt represented by samples of uncertain affiliation are presently unknown.

Radiometric ages for the subfloor basalt are almost entirely between 3.67 and 3.83 b.y. (fig. 250). The data are insufficient to strongly support or refute stratigraphic interpretations. However, all seven ages determined for samples 75035 and 75055, which are highly fractionated type A basalts from Camelot crater, have mean values of 3.76 to 3.83 b.y. This occurrence at the older end of the age range weakly supports the inference from field relations that the samples from Camelot may be among the stratigraphically lowest. No other type A basalts have been dated. The single age for a type B basalt (sample 70215) is even older, 3.84 b.y. Three ages determined for type C basalt (sample 74255 and 74275) range from 3.70 to 3.83 b.y., completely overlapping the range reported for the Camelot blocks.

Rhodes and others (1976) concluded that the well defined basalt types A, B, and C are not related to each other by low-pressure crystal fractionation but are derived from separate parent magmas whose trace-element distributions require derivation from chemically distinct parts of a heterogeneous source.

Models of possible source region characteristics have been reviewed by Papike and others (1976). Briefly, they are (1) the cumulate model, in which the basalt was generated by partial melting of cumulate rocks formed as complements to the feldspathic crust in the early melting and differentiation of the outer 1,000 km of the Moon; (2) the primitive source model, wherein the basalt was generated by partial melting of undifferentiated primitive lunar material equivalent in composition to the bulk composition of the Moon; and (3) the assimilative model, in which low-titanium melt was generated in primitive lunar material inferred, in this model, to exist below 400 km. High-titanium basalt is inferred to have been generated by assimilation when the low-titanium basaltic liquid passed through the cumulate zone below the feldspathic lunar crust.

VOLCANIC ASH

Weakly coherent material consisting of orange glass

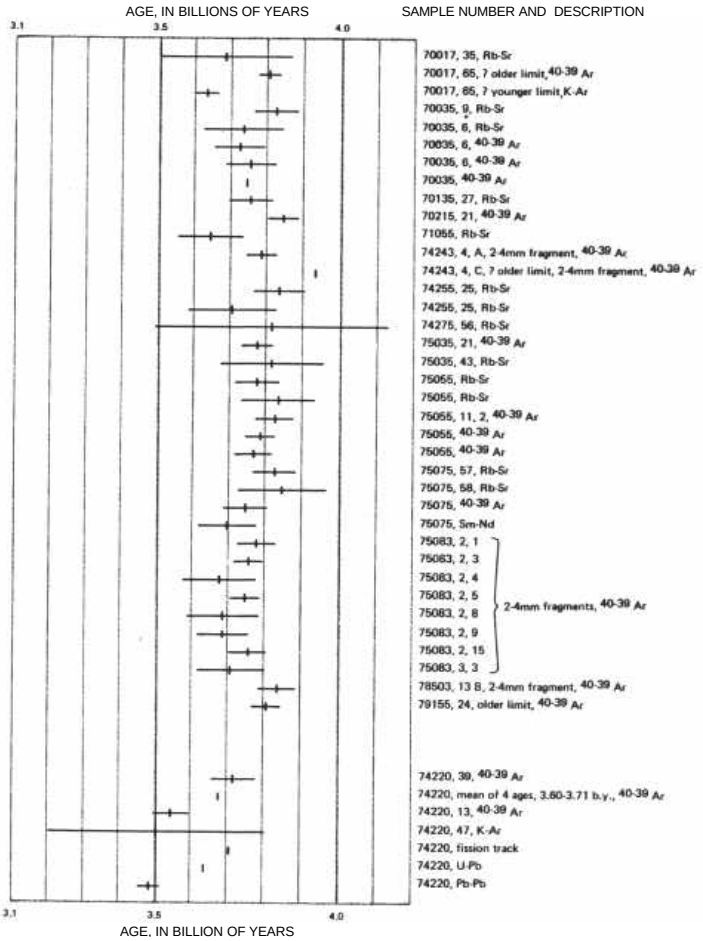

FIGURE 250.- Published radiometer ages for samples of subfloor basalt and volcanic ash. See individual sample discussions for sources of data.

beads was sampled in a trench on the rim of Shorty crater. Color photographs show that the sampled area is one of several patches of orange "soil" on the rim and walls of Shorty. The orange material exposed in the trench is 80 cm wide and may extend for several meters parallel to the axis of the rim crest. It is bounded laterally by gray sediment that represents valley-floor regolith material. A 70-cm drive tube placed in the axial part of the colored zone bottomed in a deposit of opaque black glass beads; the contact between the orange and black glass beads is apparently at about a 25-cm depth in the drive tube.

Heiken and others (1974) described the black and orange materials as well-sorted droplets ranging in size from less than 1 ,um to about 1 mm; mean grain size is about 40um. The orange droplets consist of homogeneous orange glass. A few contain olivine phenocrysts, and nearly half are partly or completely crystallized to ilmenite or intergrown ilmenite and olivine. The black droplets are partly to completely crystallized equivalents of the orange glass droplets. No droplets contain lithic debris or shocked crystal fragments.

The orange and black droplets show striking chemical homogeneity. The bulk sample (74220) from the rim of Shorty crater is much more mafic than the subfloor basalt and is distinctly different in trace-element composition (Apollo 17 PET, 1973). Citing the chemical and petrographic homogeneity and the absence of lithic and shocked crystal fragments, Heiken and others (1974) concluded that the glass beads were introduced as a pyroclastic deposit produced by fire fountaining near the edge of Mare Serenitatis. The deposit represents a magma distinct from that which formed the underlying subfloor basalt.

We interpret the patches of orange material on the rim and walls of Shorty crater as clods of ejecta excavated from a unit of volcanic ash in the Shorty target area (fig. 242). The dimensions of the sampled patch suggest that the unit of ungardened ash in the target must once have been at least 70 cm thick. That the sampled clod represents a once-widespread sheet is suggested by the ubiquitous occurrence of orange and black droplets in all of the valley-floor regolith samples (Heiken and McKay, 1974).

Even greater regional extent of the ash is indicated by telescopic spectral mapping. The Apollo 17 landing site lies within an area that was previously mapped as dark-mantle material (Scott and Carr, 1972) near the southeastern edge of Mare Serenitatis. Adams and others (1974) showed that this area is characterized by abnormally high ultraviolet and near-infrared reflectance. They found that the black droplets from Shorty crater have a unique reflectance spectrum that is also characterized by high reflectance in the ultraviolet and near-infrared and concluded that regolith in the spectrally distinct region. contains a significant black droplet component. Albedo data of H. E. Holt (Muehlberger and others, 1973) also suggest that dark material, most probably the black droplets, has been added to impact-generated basaltic and highlands regolith in an extensive area, including the landing site, near the southeastern edge of Mare Serenitatis. Such regolith, darkened by admixed ash, is the so-called dark mantle. Its distribution is the basis for mapping the extent of the volcanic ash (pl. 1).

Heiken and others (1974) , citing the occurrence of basalt fragments on the Shorty crater rim, suggested that the ash unit was rapidly buried after its deposition, either by later basalt flows or by a large ejecta blanket, protecting the materials sampled at Shorty crater from the solar wind and micro meteorites. It seems probable to us, however, that basalt flows do not overlie the ash. Shorty excavated clods of volcanic ash from within about 14 m of the precrater surface. A basalt flow that overlies the ash in the Shorty target area would occupy a significant part of that 14-m interval. The largest block seen on the Shorty crater rim is about 5 m across. Excavation of basalt from a 5m-thick flow overlying the volcanic ash would most probably be recorded by an abundance of basalt blocks on the crater rim and walls. Although a few basalt blocks do occur, the wall, rim, and flank materials of Shorty are predominantly unconsolidated fine-grained material, which suggests that no such flow is present. Furthermore, in topographic profiles of Shorty and other craters, we have recognized no evidence to suggest that a coherent basalt overlies relatively incoherent ash in the interval between the surface and the crater floors.

Another line of reasoning also favors the occurrence of the volcanic ash above the youngest subfloor basalt. In 19 samples of dark regolith material from the valley floor (LM area, station 1, LRV-3, station 4 excluding the nearly pure ash of trench sample 74220 and drive tube 74001, station 5, LRV-7, LRV-8, and station 9), the ubiquitous orange and black droplets average 10.6 percent and reach nearly 20 percent of the 90-150-,um fraction (Heiken and McKay, 1974). In addition, interpretation of spectral data indicates that they occur in the regolith over a much broader area than the landing site proper (Adams and others, 1974). Their significant abundance and widespread occurrence in the regolith, which imply that the ash was easily accessible to impact gardening over a wide area, are better explained by the occurrence of the glass-bead unit above, rather than below, the youngest subfloor basalt flows.

Many of the impact craters that formed since the volcanic ash was deposited extended downward into the

underlying subfloor basalt. Therefore, the ash now occurs only as discontinuous remnants (fig. 242).

The original thickness of the ash can be estimated only indirectly. It must be at least as great as the minimum dimension of the clods of ash on the Shorty crater rim (presumably greater than 70 cm), and it must be less than the combined thickness of ash and valley-floor regolith.

Craters with flat floors or central mounds have been formed experimentally in targets where unconsolidated material overlies coherent material; the difference in elevation between the precrater surface and the crater floor in such craters is approximately equivalent to the thickness of the unconsolidated layer (Oberbeck and Quaide, 1967; Quaide and Oberbeck, 1968). Profiles were made by analytical stereoplotter of all flat-floored or central-mound craters that we could identify on orbital panoramic camera photographs of the Taurus-Littrow valley floor. For 39 of the 40 craters profiled, the measured difference in elevation between the estimated precrater surface and the floor is between 5 and 28 m; approximately three-fourths are clustered at values from 8 to 17 m (fig. 251). The mean for the entire group is about 14 m.

Profiles show that the floors of Van Serg, Shorty, and Gatsby craters are respectively about 11, 14, and 17 m below their estimated target surfaces. Crew observations, lunar surface photographs, and returned samples suggest that the Van Serg impact did not excavate subfloor basalt at 11 m and that Shorty crater may have just reached the subfloor basalt at 14 m (Muehlberger and others, 1973; Apollo Field Geology Investigation Team, 1973; Schmitt, 1973). Enlarged panoramic camera photographs show nearly a dozen meter-size or larger blocks in and near Gatsby crater, which suggests that Gatsby excavated subfloor basalt at a depth of about 17 m. Abundant large blocks are visible in and around most of the craters larger than Gatsby.

The data from Van Serg, Shorty, and Gatsby as well as from the 40 crater profiles suggest that 14 m is a reasonable estimate for the average thickness of unconsolidated material above the subfloor basalt. The results of the active seismic experiment are permissive with respect to this estimated average. Cooper and others (1974) have offered two models based on the seismic data: (1) The top of the basalt is at a depth of 7-12 m, and (2) the top of the basalt is at a depth of 32 m.

If the average proportion of orange and black droplets measured by Heiken and McKay (1974) in dark regolith samples of the valley floor (10.6 percent) is representative of the proportion of ash in the 14-m average thickness of unconsolidated deposits, it implies that a minimum thickness of the original ash bed was

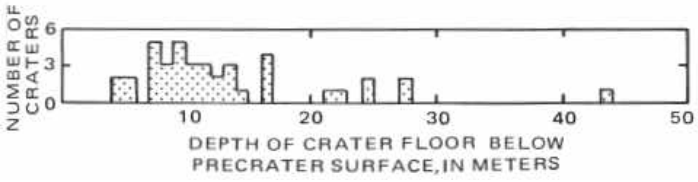

FIGURE 251.-Elevation differences between precrater surfaces and floors of flat-floored or central-mound craters. (From Wolfe and others, 1975.)

approximately 1.5 m. Two observations suggest that the original thickness was greater than 1.5 m: (1) The occurrence of clods of pure ash in the ejecta of Shorty crater shows that not all of the original ash deposit has been mixed into the regolith, and (2) the impacts that formed the many large fresh craters in the landing area (pl. 2) excavated deep into the subfloor basalt. The widespread ejecta of these craters is relatively enriched in basalt debris, hence relatively poor in volcanic ash. Therefore, the 10.6-percent average is probably a minimum value for the average proportion of volcanic ash in the unconsolidated deposits of the valley floor.

The regolith at the Apollo 11 site, developed on basalt similar in composition and age to the subfloor basalt, is 3 to 6 m thick (Shoemaker and others, 1970). An equivalent thickness probably would have formed on the subfloor basalt at Taurus-Littrow if there were no other contributing sources. However, the nearby highlands have provided a large amount of debris to the valley floor (figs. 245 and 246), perhaps enough to increase the regolith thickness 5 to 10 m. Given an average combined thickness of 14 m, we can speculate that the original ash thickness was 4-9 m. Much of that ash has been reworked by impact gardening so that it now occurs as a component of the regolith.

Radiometric age measurements (fig. 250) support the hypothesis that the ash overlies the youngest subfloor basalt. Mean ages determined for the ash range from 3.48 to 3.71 b.y. Hence they overlap a few of the younger ages determined for the subfloor basalt. Ages determined for large blocks of basalt (samples 74255 and 74275) on the rim of Shorty, which may represent the stratigraphically highest basalt included among the samples, range from 3.70 to 3.82 b.y., barely overlapping the range of ages for volcanic ash sample 74220.

Tera and Wasserburg (1976) determined a Pb-Pb age of 3.48±0.03 b.y. for carefully separated and cleaned glass spheres. They suggested that Ar entrapment and Pb contamination by components other than orange glass in sample 74220 were responsible for the greater ages determined by other investigators. All Apollo 17 basalt ages determined so far are distinctly older than this 3.48 b.y. age for the volcanic ash (fig. 250).

A dark mantle with local orange and red material has been described in the Sulpicius Gallus region at the

southwest edge of Mare Serenitatis (Lucchitta and Schmitt, 1974). It has low albedo and an unusually smooth surface like the smooth dark surface of the so called dark mantle of the Taurus-Littrow region (Lucchitta, 1973). Presumably it also represents a deposit of volcanic ash (Head, 1974c; Lucchitta and Schmitt, 1974), and it could be correlative with the ash of the Apollo 17 area. As in the Taurus-Littrow region, the Sulpicius Gallus dark mantle occurs on older highly faulted mare basalts. Younger, lighter appearing basalt of Mare Serenitatis overlaps the faulted basalt and its mantling ash deposits in both regions (pl. 1; Howard and others, 1973). On the basis of crater morphology, Boyce (1976) has estimated the age of the younger lava in the southern part of Mare Serenitatis at 3.4±0.1 b.y.

The abnormal thickness of unconsolidated ash bearing material overlying the subfloor basalt resulted in the formation of a relatively smooth dark surface, interpreted before the mission as the manifestation of a very youthful dark mantling deposit. Statistical crater studies (Lucchitta and Sanchez, 1975) showed that large craters (diameter greater than 175 m) are more abundant on the dark surface than on the lighter surface of Mare Serenitatis, a result in accord with the age differences interpreted on photogeologic grounds. However, there is a marked deficiency of craters in the 100-200-m size range on the dark-mantled surface; the density of craters in this size range is less than half that on the light mare surface. As an alternative to the now untenable hypothesis that the smaller craters were buried by a younger dark mantle deposit, we suggest that they have been degraded beyond recognition at an abnormally high rate because they formed in an abnormally thick layer of unconsolidated material. Their counterparts in age and size on Mare Serenitatis, where normally thin regolith overlies mare basalt, have been well preserved because the volumes of those craters are largely within basalt rather than within soft ash and regolith.

REGOLITH

Impact-generated regolith of the Taurus-Littrow valley is a mechanical mixture that consists largely of debris derived from the highlands, from the subfloor basalt, and from the volcanic ash. Chemical compositions of regolith material (figs. 245, 246) form a continuum from the nearly pure highlands material of station 2 and the light mantle to the basalt-rich regolith of the LM area and stations 1 and 5. Geologic relations in combination with compositions enable us to distinguish highlands regolith and three major valley-floor units: (1) older regolith of the valley floor, (2) cluster ejecta, and (3) light mantle (fig. 242). A plot showing relative amounts of $Ti0_2$, $A1_20_3$, and FeO+MgO in sediment samples (fig. 245) suggests that highlands material makes up more than 50 percent of sediment collected at highlands and light-mantle stations, approximately 33 to 50 percent of sediment in the older valley-floor regolith, and less than 33 percent in samples of cluster ejecta. A second plot (fig. 246), showing relative amounts of CaO, MgO, and FeO, shows an almost identical distribution of data points, except that the apparent proportions of highlands component are slightly lower. Boundaries between the three groups of regolith samples have been drawn in figure 246 at positions equivalent to approximately 45 and 25 percent highlands material.

HIGHLANDS REGOLITH

Nearly pure highlands regolith is exemplified by the sediment samples from station 2 at the base of the South Massif and station 2a on the nearby surface of the light mantle. The compositions of these samples approximate a mixture of the two major components of the massif (fig. 244), breccia matrix material (noritic breccia of figures 245 and 246) and feldspathic plutonic or metaplutonic rocks (anorthositic gabbro of figures 245 and 246), and a small amount of basalt and ash debris from the valley floor. Heiken and McKay (1974) recognized a few percent of ash and basalt in the 90-150-,um fraction in these particular samples. Rhodes and others (1974) suggested on chemical grounds that they contain, on the average, about 6 percent ash 2 percent basalt, and approximately equal amounts of noritic breccia and anorthositic gabbro. The near absence of valley-floor material at station 2 and the chemical similarity between regolith samples from stations 2, 2a, and 3 (figs. 245 and 246) suggest that the light mantle may completely cover the surface in the station 2 area.

At stations 6, 7, and 8, at the bases of the North Massif and Sculptured Hills, the sediment compositions reflect the addition of a large valley-floor component. Such an admixture is to be expected close to the mare-highlands boundary and may be enhanced at these particular stations, which we interpret as downrange from the abundant clustered craters of the valley floor. Subfloor basalt fragments, included among the samples from stations 6, 7, and 8, are all presumably ejecta fragments from craters of the valley floor.

The data points for stations 6 and 8 are near or coincident with the join drawn between the volcanic ash and highlands compositions in the triangular diagrams (figs. 245, 246). Possibly volcanic ash reworked from the surfaces of the North Massif and Sculptured Hills is a major component at these stations. For station 8 in particular this would be in agreement with the photograph

geologic observation that the station is in an area of dark smooth surficial material. However, orange and black glass are relatively minor components of the 90-150-um sediment fractions at these stations (Heiken and McKay, 1974). Debris from magnesium-rich norite similar in composition to samples 78235 and 78527 from station 8 or, to a lesser extent, debris from the noritic massif matrix material would also tend to drive the sediment compositions toward, if not below, the highlands-volcanic ash join.

OLDER REGOLITH OF THE VALLEY FLOOR

The older regolith of the valley floor is debris generated by impact processes over the long period (~3.5 b.y.) between emplacement of the volcanic ash and the much more recent formation of the cluster ejecta and light mantle. Samples include sediment and regolith breccia from ejecta on the rim of Van Serg crater (station 9), gray ejecta from the trench on the rim of Shorty crater (station 4), sediment from the lower 2 m of the deep drill (70001-70009), and sediment collected at LRV-3. The unit is a mixture of basalt debris, ash, and highlands debris (figs. 245, 246; Heiken and McKay, 19 7 4; Rhodes and others, 1974). Highlands component makes up approximately 30 to 50 percent; hence, the older regolith unit is intermediate within the compositional continuum from highlands and lightmantle sediment to basalt-rich cluster ejecta. Its thoroughly mixed character implies a long history of homogenization of ejecta derived largely from the local highlands, the subfloor basalt, and the volcanic ash.

CLUSTER EJECTA

The uppermost part of the regolith in the area of the LM and stations 1 and 5 consists of basalt-rich sediment with significant but subordinate admixtures of highlands debris and ash (figs. 245 and 246; Heiken and McKay, 1974; Rhodes and others, 1974). The base of this unit, denoted here as the cluster ejecta, occurs between 30 and 93 cm depths (approximate positions of the analyzed samples denoted 70008 and 70006, respectively, in fig. 10) in the deep drill stem. The petrography of samples from deep drill segment 70008 (Heiken and McKay, 1974) suggests that basalt-rich sediment may extend downward at least as far as the 59-cm depth (sample 70008,239). Curtis and Wasserburg (1975b) suggested from their evaluation of neutron fluence that a uniform and distinctive shallow interval is represented in approximately the upper 60-70 cm of the deep drill stem. The abundance of basalt debris suggests that this distinctive unit is dominated by ejecta from craters large enough to have excavated subfloor-basalt bedrock. Such craters form the large cluster in the landing area (pl. 2) . They are part of a system, including many smaller craters, that is also present on top of the South Massif and in the northern highlands. Figure 252 shows its extent in the Taurus-Littrow area and delineates the areas most heavily affected on the valley floor.

Camelot crater and the three craters Henry, Shakespeare, and Cochise near the north edge of the Taurus-Littrow valley appear more degraded and therefore were previously interpreted as older than the prominent clustered craters south and east of the LM (for example, Lucchitta, 1972; Wolfe and others, 1975). However, topographic profiles made by analytical stereoplotter show that the depth-to-diameter ratio of Camelot crater is similar to that of the larger craters south and east of the LM. Hence, we now regard Camelot as part of the large cluster outlined in figure 252.

Depth-to-diameter ratios for the three northern craters are less than those of large craters east and south of the LM. Perhaps the three craters formed where colluvium from the North Massif was relatively thick; that is, coherent subfloor basalt was more deeply buried in the targets for the Henry, Shakespeare, and Cochise impacts than it was for craters near the center of the valley. If so, their more subdued forms may reflect relatively greater thickness of incoherent target material rather than relatively greater age. We now tentatively also include the three northern craters in the extensive crater cluster (fig. 252).

The relatively youthful appearance of the craters south and east of the LM in comparison with Camelot, Henry, Shakespeare, and Cochise may be due to the abundance of smaller craters, also part. of the cluster, that have sculptured the walls, rims, and ejecta blankets of the larger craters. Camelot and the three northern craters differ because of the absence of abundant smaller associated craters. Hence, they have smoother looking rims and ejecta blankets.

A large part of the traverse area is pitted by the clustered craters and covered by their ejecta. A theoretical ejecta distribution calculated by Lucchitta and Sanchez (1975) for the larger craters (fig. 253) suggests that cluster ejecta occurs widely on the valley floor. This distribution is based on the equation of McGetchin, Settle, and Head (1973): $T=0.04\,R$, and $t=T(r/R)^{-3.0}$, where T is thickness of ejecta at the crater rim, R the radius of the crater, and t the thickness of ejecta at a distance r, measured from the center of the crater. The distribution shown in figure 253 should be construed only as a theoretical approximation. However, it predicts a thickness of cluster ejecta at the deep-drill site that is in reasonable agreement with the observed thickness of basalt-rich sediment in the upper part of

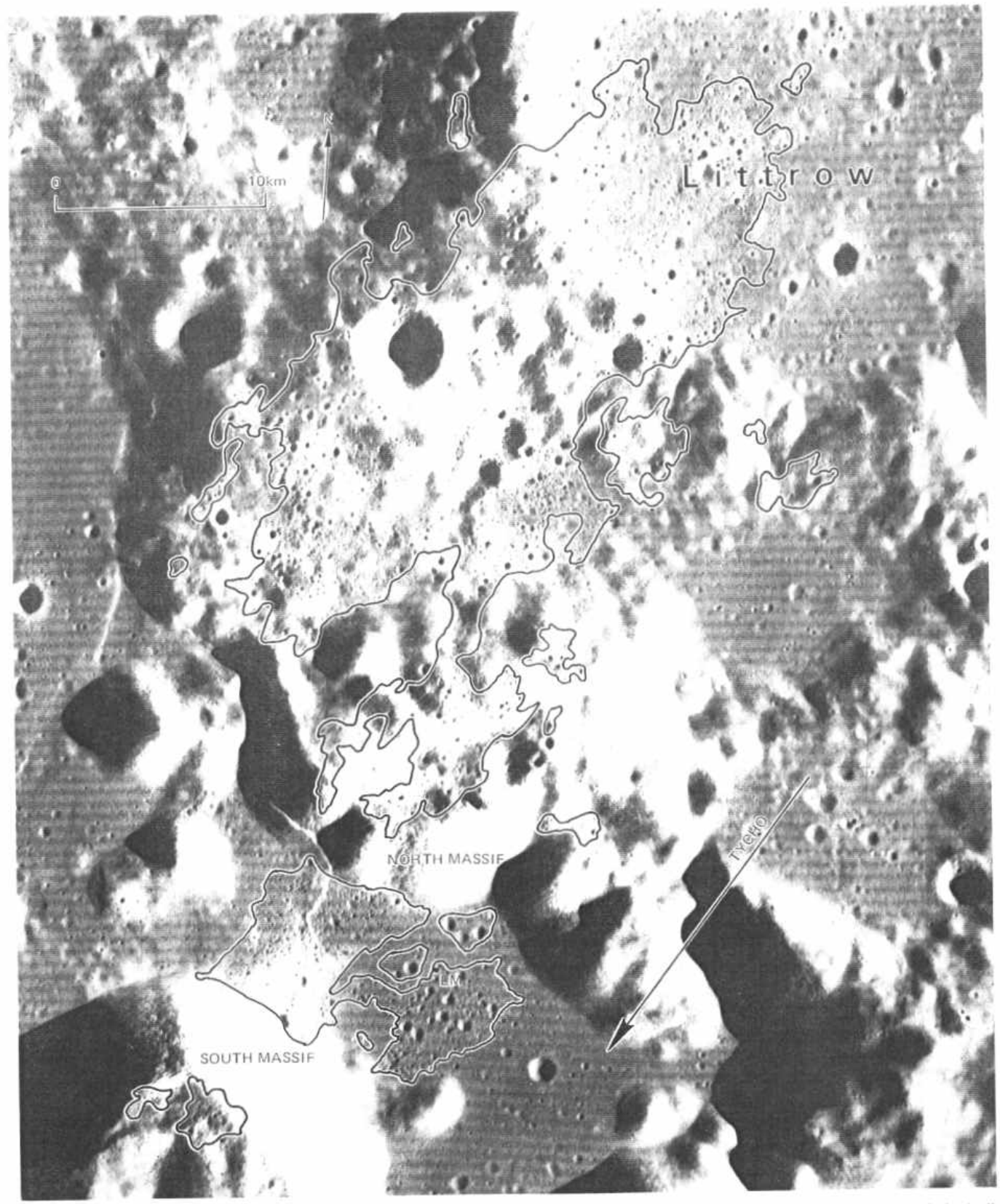

FIGURE 252.-Areal distribution clustered craters in Taurus-Littrow area. Cluster is alined toward Tycho, and craters are morphologically like Tycho secondary - craters. (Modified from Lucchita, 1977; NASA photograph M- 17-447.)

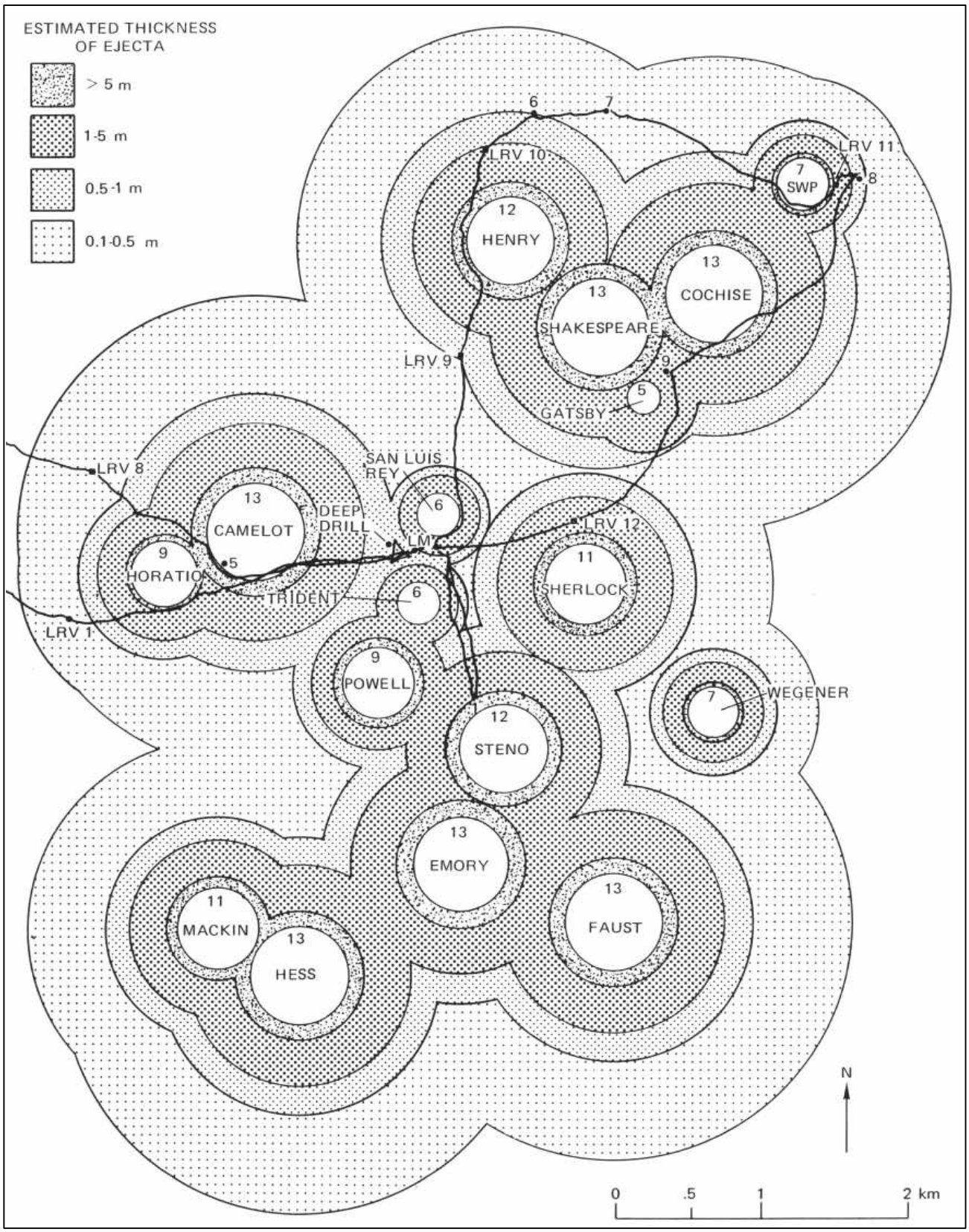

FIGURE 253.-Theoretical distribution of ejecta from larger craters in Apollo 17 landing area. Number within each crater shows theoretical thickness (in meters) of ejecta at crater rim. Aggregate thickness of overlapping ejecta blankets is not portrayed. (Adopted from Lucchitta and Sanchez, 1975.)

the drill core.

Exposure ages determined for samples from large basalt boulders in the LM area range from 95 to 106 m.y. The boulders are best interpreted as part of the cluster ejecta. Samples from the two half-meter boulders from the rim of a fresh 10-m crater at station 1 have exposure ages of 102 and 110 m.y. They are probably ejecta fragments from Steno crater that were excavated, or at least repositioned, by the impact that formed the 10-m crater. The approximate equivalence of the station 1 exposure ages to those" of the LM-area boulders suggests that the station 1 boulders were not significantly shielded before the 10-m crater was formed. These data suggest that the cluster ej ecta was deposited about 100 m.y. ago. Carefully selecting samples for which they interpreted simple exposure histories, Arvidson and others (1976b) calculated a mean age of 96±5 m.y. for the clustered craters.

Samples of the three large boulders of highly fractionated basalt from the rim of Camelot crater have exposure ages ranging from 70 to 95 m.y. The 70-m.y. date is a track age determined for sample 75055. Three argon ages for the same sample range from 85 to 95 m.y., in approximate agreement with the data from the LM area and station 1. Sample 75015 gave an exposure age of 92±4 m.y., and sample 75035 gave ages of 72 and 80 m.y. The boulders from which these were collected may have had complex histories, possibly including catastrophic rupture to form the two boulders from a single one. Hence, the exposure ages measured for samples 75015 and 75035 may be less than the age of Camelot crater (Arvidson and others, 1976b).

In a study of secondary crater clusters over a large part of the Moon, Lucchitta (1977) found that clusters formed by projectiles from Tycho have a distinctive, easily recognized morphologic pattern. She concluded that the Taurus-Littrow cluster (fig. 252) was formed by impacts of projectiles from Tycho. Evidence includes the following: (1) Clustered craters in the Taurus-Littrow area show close morphologic resemblance to Tycho secondary clusters elsewhere on the Moon; (2) grooved and braided surfaces in the Taurus-Littrow cluster, as in other Tycho secondary clusters, are characterized by V-shaped patterns that open directly away from Tycho; and (3) the TaurusLittrow cluster is elongate in the approximate direction of a Tycho radial (fig. 252). As one would expect, no Tycho ejecta has been recognized among the Apollo 17 samples. Exposure age data summarized above suggest that the clustered craters and, presumably, Tycho were formed about 100 m.y. ago.

LIGHT MANTLE

The light mantle is a deposit of light-colored predominantly fine-grained unconsolidated material with fingerlike projections that extend 6 km across the valley floor from the South Massif (pls. 1 and 2). The unit feathers out at its margins away from the South Massif. Near the distal end, Shorty crater and a smaller nearby crater penetrate the light mantle to the underlying darker regolith material. However, near the South Massif, craters as large as 75 m in diameter do not penetrate to darker underlying material.

Rock fragments collected from the light mantle are dominantly breccia like those from the massif stations. Sediment samples from stations 2, 2a, and 3 contain no more than a few percent of basalt and ash from the valley floor. However, samples from LRV-2 and LRV-6, from thin light mantle relatively far from the South Massif, contain a significantly larger valley-floor component (figs. 245 and 246) . The highlands component of the light-mantle sediment samples is approximated by a mixture of the two major compositional groups, noritic breccia matrix material and feldspathic plutonic or metaplutonic rocks, that we recognize in the massif samples.

The composition of the light mantle, the lithologic similarity of its scattered rock fragments to samples collected at the massif stations, the general predominance of fine-grained material, and its geometric form as a raylike body extending outward from the South Massif, suggest that it consists of redeposited regolith material from the South Massif. The light mantle has been interpreted as the deposit of an avalanche triggered, perhaps, by the impact on the South Massif of secondary projectiles from Tycho (Scott and others, 1972; Howard, 1973; Muehlberger and others, 1973). Regional study of Tycho secondary crater clusters (Lucchitta, 1977) has shown that the light mantle is a local manifestation of the Taurus-Littrow crater cluster (fig. 252) and has confirmed the earlier hypothesis that South Massif regolith material was mobilized by impacting secondary projectiles from Tycho. Citing the morphologic similarity between the light mantle surface adjacent to the South Massif and the finely braided ejecta with V-shaped grooves and ridges seen downrange from Tycho secondary clusters, Lucchitta (1977) concluded that the light mantle was primarily ejecta launched from Tycho secondary craters on the crest and north face of the South Massif rather than regolith material jarred into avalanche motion. It seems most likely that the Tycho secondary impacts on the steep massif face mobilized unconsolidated regolith material in both ballistic and avalanche modes to produce the light mantle.

The light mantle is older than Shorty crater, estimated from exposure ages of crater rim materials to have formed between 10 and 30 m.y. ago. The boulders

at station 2 were probably emplaced after deposition of the relatively boulder-free light mantle. Leich and others (1975) concluded that boulder 1 has been in its present position at the base of the South Massif for about 42 m.y. If our view is correct that the light mantle and the clustered craters on the valley floor to the east were all produced by impacting projectiles from Tycho, then these features are temporally equivalent. Accordingly, Arvidson and others (1976a) included the 107-m.y. exposure age of station 2 rake-sample fragment 72535 in the group of selected exposure age data from which they calculated a 96±5-m.y. estimate for the age of the light mantle and clustered craters. We concur that the light mantle, like the cluster ejecta, is approximately 100 m.y. old.

STRUCTURAL GEOLOGY

We recognize three major groups of deformational events. In order of decreasing age, they are (1) block faulting of the highlands, (2) deformation of the mare surfaces, and (3) development of the ridge-scarp system.

BLOCK FAULTING OF THE HIGHLANDS

Some boundaries of massif blocks are linear topographic breaks that. resemble fault traces. They occur at contacts with adjacent blocks, with Sculptured Hills material, and with subfloor basalt (pl. 1). The most prominent ones, shown in figure 254, do not extend into the basalts. Some are found, however, within Sculptured Hills material.

The linear topographic breaks are presumably fault related but are not necessarily the actual fault traces, which we believe are either buried by thick wedges of colluvium (fig. 242) or mantled by Sculptured Hills material deposited after block faulting was initiated. Surfaces of the colluvial wedges or mantling Sculptured Hills deposits tend to parallel the buried fault surfaces. Some of the faulting, however, postdates deposition of the Sculptured Hills material.

Previous workers (Scott and Carr, 1972; Head, 1974a) concluded that (1) the massifs now stand where steeply dipping faults, activated during basin formation, coincide with the systematic older fractures of the lunar grid (Strom, 1964) and (2) faults in the Taurus-Littrow area may have been reactivated by the later Imbrium event. A graphic summary (fig. 255) of the bearings and cumulative lengths of the faultrelated topographic breaks (fig. 254) confirms their high degree of coincidence with the lunar grid maxima. The dominant Taurus-Littrow maximum, approximately N. 60° W., coincides with the well-defined northwest maximum of the lunar grid but differs by about 10°-15° from radials through the landing point from the Imbrium and southern Serenitatis basin centers. Hence, the dominant strike of the block faults is approximately radial to the southern Serenitatis basin, but it is skewed slightly clockwise, presumably because of the control exerted by the older fractures. Whether or not the block faults were reactivated by the Imbrium impact cannot be determined.

DEFORMATION OF-THE MARE SURFACES

A broad topographic low within mare basalt parallels the southeast margin of Mare Serenitatis (fig. 256). The deepest part of this broad trough is about 600 m lower than the central part of Mare Serenitatis, which is located near lat 24.5° N., long 18° E. It is also more than 1,800 m lower than the mare surface near the crater Vitruvius in the southeast corner of plate 1. Stratigraphic relations suggest that the two older Imbrian basalt units (lb_1 and Ib_2) are successively overlapped downslope toward the trough axis by the two younger Imbrian units (Ib_3 and Ib_4) (fig. 256). The older basalts are characterized by relatively rough surfaces compared to the younger lavas and are marked by deep linear and sinuous rilles, faults, and collapse depressions having different sizes and shapes. The overlap relations are best shown in the wide reentrant extending southeast between the craters Dawes and Fabbroni, where all four units are exposed. Along the shelflike eastern margin of Mare Serenitatis west of the crater Clerke, the youngest basalt (unit Ib_4) has presumably completely overlapped the second youngest (Ib_3) and embays the third youngest unit (Ib_2) (fig. 256).

The mare surfaces continue to rise southeast outside the map area into the Tranquillitatis basin; overall relief measured from the axis of the Serenitatis trough is nearly 3 km. If the oldest and topographically highest basalt unit (Ib_1) originally had an approximately horizontal upper surface and if it is buried by the younger basalts beneath the axis of the synclinal trough, then a minimum of about 3 km of structural relief (more than 2 km within the map area) has been developed on it. This is a minimum figure and does not take into account the thickness of the overlying basalt flows within Mare Serenitatis. Gravity data indicate that an excess mass distribution of 1,050 kg/cm2 is present on the floor of Mare Serenitatis (Sjogren and others, 1974a). If the basin was isostatically compensated before extrusion of the mare basalts, the excess mass could represent a superisostatic load equivalent to an average thickness of between 3 and 4 km of basalt. If the basin cavity was not compensated, however, the density contrast between basalt and anorthositic terra material, probably about 0.4 g/cm3 (Kaula, 1975), should be used in calculating the basalt thickness. This would amount to a basalt fill of about 25 km. A smaller es

FIGURE 254.-Major linear topographic breaks in Taurus-Littrow highlands. Although some may coincide with traces of faults, most are probably offset from faults that they parallel by colluvial deposits or by mantling Sculptured Hills material. (NASA photograph M-17-1219.)

timated density contrast would result in a proportionally greater hypothetical thickness. The actual thickness of fill probably lies somewhere between these two extremes. In any case, a total relative uplift of several kilometers must have occurred, provided the basalts had initially level upper surfaces.

Some of the older basalt units (lb_1, Ib_2, Ib_3) may have originated partly from within the Tranquillitatis basin and flowed downslope into Serenitatis. The upper contact between the second and third oldest (Ib_2 and Ib_3 respectively) units, for example, is very uncertain (pl. 1) , and the younger unit (Ib_3) may extend farther southeast or southwest. The long sinuous rilles of the third oldest (Ib_3) unit, within the reentrant in the southeastern part of the map area, indicate that this basalt flowed down a sloping older mare surface. These rilles are interpreted to be collapsed lava tubes or lava channels requiring the fluid flow of basalt during their formation. As these rilles extend directly downslope nearly normal to the topographic contours, it seems reasonable that the basalt unit in which they occur had an initial slope in the same direction, if not of the same magnitude as the present surface in this area.

The mare basalts and plains material in the vicinity of the Apollo 17 landing area (Muehlberger, 1974) have been warped into a broad flat-topped arch. The axis of this fold lies between the craters Clerke and Littrow and extends south toward Mons Argaeus near the crater Fabbroni (fig. 256). This arch is expressed neither in the younger basalts north of Clerke nor in the older flows south of Mons Argaeus. Its faulted west limb is overlapped by the younger basalt (Ib_4) of Mare Serenitatis (pl.1).

A sinuous depression north of Mons Argaeus (pl. 1) crosses the southern part of the arch. If the depression represents a lava channel or tube within the secondoldest unit (Ib_2) it has been deformed by development of the arch so that lava flowing northward in its southern part would now have to flow uphill for the first 10 km before beginning its descent northwestward toward Mare Serenitatis.

Formation of the marginal trough in eastern Mare

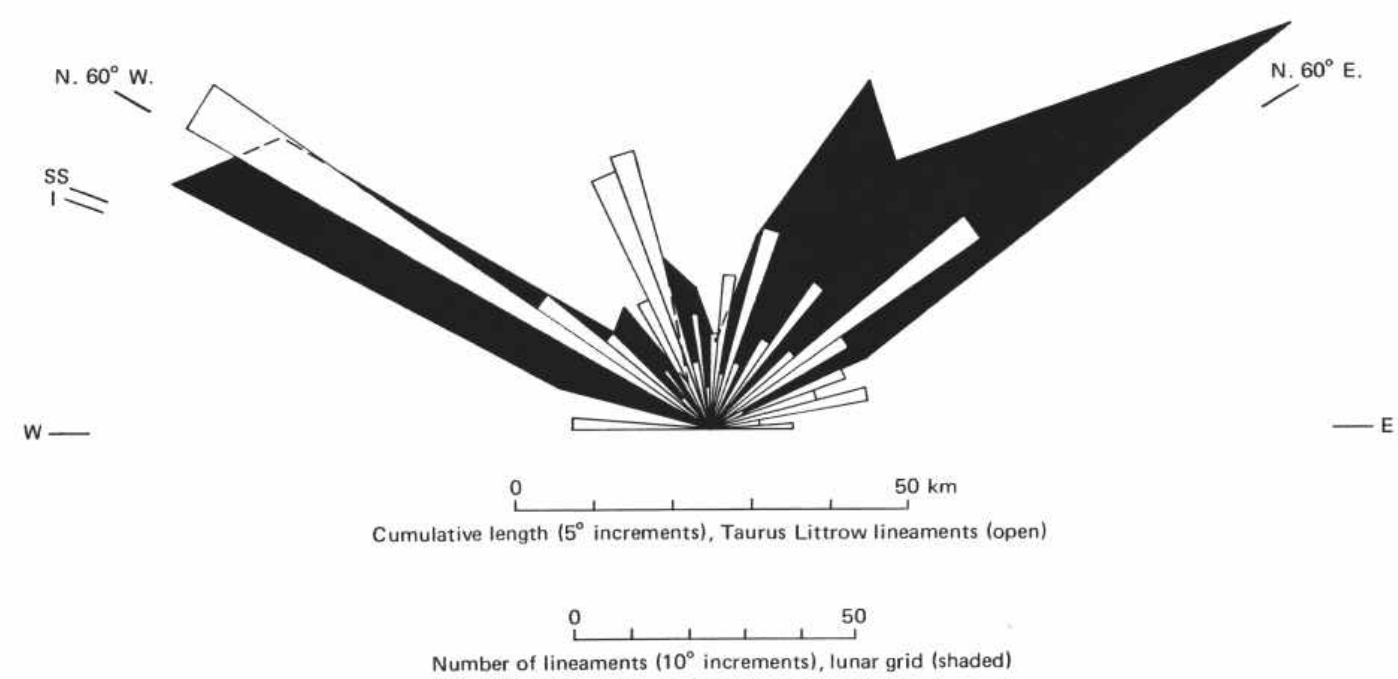

FIGURE 255.-Cumulative lengths in 5° increments of lineaments of figure 254 (open pattern). Shaded pattern is Strom's (1964) azimuth-frequency diagram of lineaments in part of the Moon's northern hemispere. SS, I, azimuths of radials through Apollo 17 landing point from centers of southern Serenitatis and Imbrium basins, respectively. Southern Serenitatis basin center, 24.5° N., 18° E. (Scott, 1974); Imbrium basin center, 37° N. 19° W. (Stuart-Alexander and Howard, 1970).

Serenitatis (fig. 256) postdates the emplacement of all the mapped basalt units. The youngest basalt unit (M) extends from the basin center outward (east) across the axis of the trough (fig. 256). Its contact with underlying flows does not follow the present topography within the low region, as would be expected if folding

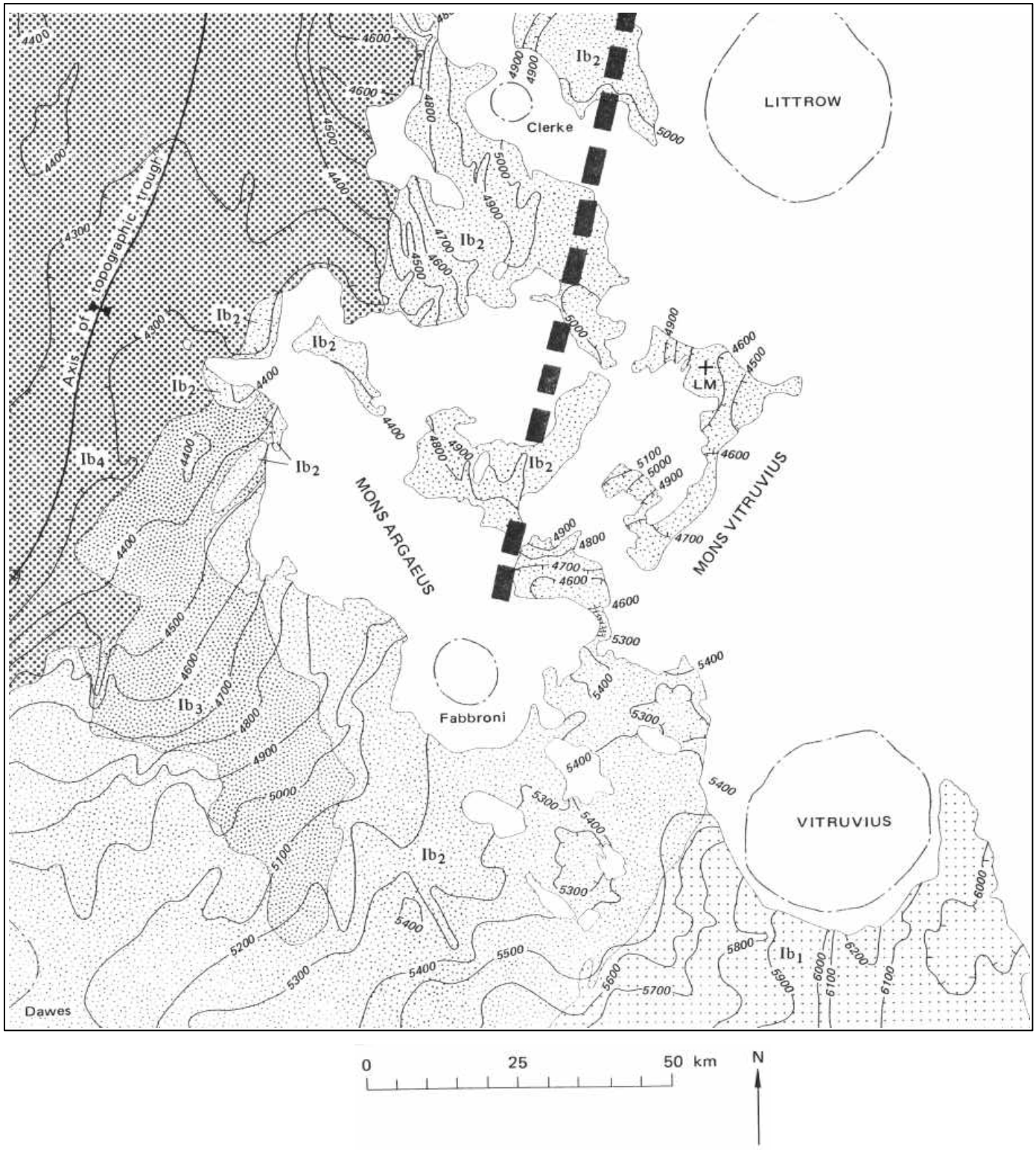

FIGURE 256.-Topographic contours on mare basalt units (Ib_1-Ib_4) of Taurus-Littrow region (Ib_1, oldest; Ib_4, youngest). Heavy broken line is approximate crest of broad flat-topped arch of Muehlberger (1974). Contours generalized from National Aeronautics and Space Administration Lunar Topographic Orthophotomaps LTO42C2,3; LT043D1,4. Contour interval is 100 m.

had occurred before its extrusion.

DEVELOPMENT OF THE RIDGE, SCARP SYSTEM

The Lee-Lincoln scarp is the easternmost of a broad band of wrinkle ridges and scarps that transect mare and highlands in the Taurus-Littrow area. They extend south-southeast from Mare Serenitatis and the adjacent highlands near the crater Clerke almost to the crater Vitruvius (pl. 1).

North of the Taurus-Littrow valley, on the North Massif and in the Sculptured Hills unit between the North Massif and Clerke (pl. 1), the Lee-Lincoln system extends as well-defined single nearly linear east- to northeast-facing scarps arranged en echelon. They generally trend nearly north, but one segment parallels the south edge of the North Massif. This segment may follow the trace of the older massif-bounding fault, which may have been reactivated so as to break the colluvial wedge during formation of the Lee-Lincoln scarp (Head, 1974a; Wolfe and others, 1975).

On the valley floor the Lee-Lincoln scarp resembles an asymmetrical mare ridge. The east-facing scarp, up to about 80 m high, consists of irregular, imbricate, and overlapping lobes (pl. 2; figs. 6, 7A, B).

The scarp cuts the crater Lara and is overlain by the light mantle. Therefore the main movement took place between the formation of Lara and deposition of the light mantle. However, a few fresh-looking scarplets may cut the light mantle, which suggests that some movement may have occurred relatively recently (100 m.y.). In addition, the light mantle is cut by a system of fresh high-angle faults and grabens located 2 to 3 km west of the Lee-Lincoln scarp and trending approximately parallel to it (pl. 2).

Hypotheses attributing the formation of mare ridges to volcanic processes, tectonic processes, and combinations of the two were reviewed by Lucchitta (1976). She concluded that the wrinkle ridges and related highland scarps, including specifically the Lee-Lincoln system, were formed by faulting for three reasons. (1) Mare ridges cross stratigraphic units of differing age (pl. 1), including the rims of craters that are much younger than the underlying mare units (for example, an unmapped 2.5-km crater near the south end of Dorsa Aldrovandi on pl. 1; Lara crater on pl. 2 and fig. 7A); hence, they are not primary constructional features of the units on which they occur. (2) The Lee-Lincoln system continues from mare materials of the valley floor into highlands material of the massifs and Sculptured Hills, where it resembles a simple system of faults, up on the west. (3) No fragments of volcanic rock sufficiently young to support a hypothesis of volcanic origin for any part of the Lee-Lincoln system have been found in the Apollo 17 samples.

In a detailed topographic analysis, Lucchitta (1976) found that a fault plane at the base of the Lee-Lincoln scarp would generally be nearly vertical and that more segments have dips that indicate reverse faulting than normal faulting. However, fresh small grabens and high-angle faults that parallel the scarp 2 to 3 km to the west (pl. 2) indicate that tensional stress may have been present locally. These relations are compatible with a model in which local extension and local shortening result from vertical tectonic movements (Sanford, 1959). Normal faults may develop over relatively raised areas and reverse faults over relatively depressed areas (fig. 257).

The cause of these vertical movements is not clear. Muehlberger (1974) interpreted the mare-ridge structures as wrinkles in the surface as a result of global compression. Other investigators have considered them to be the result of crumpling due to gravitational settling of the mare surface into a reduced space (Bryan, 1973; Maxwell and others, 1975). Another possibility is that the tectonic effects result from long-term isostatic adjustments related to basin formation or to the redistribution of lunar mantle material when the voluminous mare basalts were generated and extruded. Whatever the reason, such adjustments apparently have continued into relatively recent (post dating the light mantle) time as minor episodic faulting.

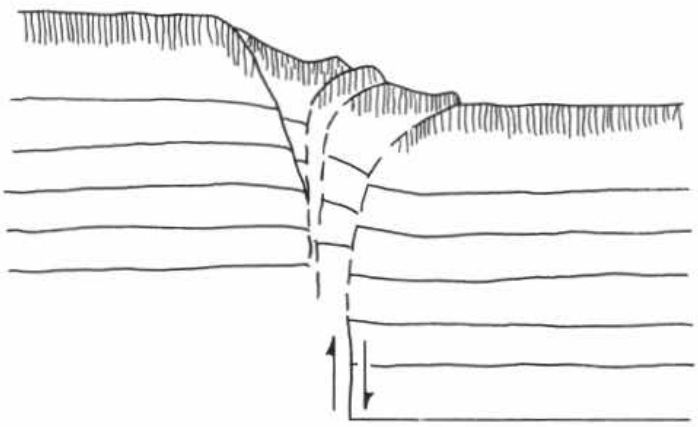

FIGURE 257.-Schematic cross section showing how morphology of Lee-Lincoln scarp on Taurus-Littrow valley floor might result from high-angle faulting of subfloor basalt. Sketch after drawings by Sanford (1959). Note normal faulting under tension over relatively raised block and reverse faulting on relatively lowered block from Lucchitta, 1976).

REFERENCES CITED

Adams, J. B., Pieters, C., and McCord, T. B., 1974, Orange glass Evidence for regional deposits of pyroclastic origin on the Moon, *in* Proceedings Fifth Lunar Science Conference, v. l: Geochim. et Cosmochim. Acta, Supp. 5, p. 171-186.

Albee, A. L., Dymek, R. F., and DePaolo, D. J.,1975, Spinel symplec tites-High-pressure solid-state reaction or late-stage magmatic crystallization?, in Lunar Science VII, Abstracts of papers